Stockholm School of Economics
Department of Economics
5350 Master's thesis in economics
Spring 2026

Swedish Breakeven Inflation: Estimating Inflation Expectations and Risk Premia

Sten Almgren (42855) and Nils Dahl (42842)

Abstract: This thesis adopts an affine term structure model that jointly prices the nominal and inflation-linked term structures for Swedish government bonds. We estimate the expected inflation, inflation risk premium and liquidity premium components in breakeven inflation rates (BEI) from 2-year to 10-year maturities. We find that changes in Swedish BEI is primarily caused by changes in risk premia, with time varying inflation risk premia contributing to most of the variation, especially at longer horizons. Our results suggest that BEI is a noisy measure of inflation expectations, particularly in periods of market stress, and should be interpreted with caution when assessing inflation outlooks and monetary policy credibility.

Keywords: Affine term structure model, breakeven inflation, expected inflation, inflation risk premium, liquidity premium

JEL: E43, E44, G12

Supervisor:	Rickard Sandberg
Date submitted:	18.05.2026
Date examined:	...
Discussant:	Soumya Sahoo
Examiner:	Sampreet Singh Goraya

Acknowledgements

We would like to express our sincere gratitude to our supervisor, Rickard Sandberg, for his valuable advice and support throughout the research process.

AI Declaration

During the preparation of this thesis, we made use of AI-based tools, primarily Claude and ChatGPT. These tools were mainly used to support coding tasks, such as understanding how to implement specific steps, debugging, and correcting syntax errors. In addition, they were used to improve the language, and readability of the written text. The use of these tools was strictly supportive, and all analytical work, interpretations, and conclusions are our own.

Contents

1 Introduction **3**

2 Background and related literature **4**

3 A joint nominal and inflation-linked no-arbitrage affine term structure model **7**
- 3.1 Risk neutral no-arbitrage bond pricing . . . 8
- 3.2 Real bonds . . . 10
- 3.3 Break-even inflation decomposition . . . 11
- 3.4 Inflation-linked bonds . . . 12

4 Parameter estimation **12**
- 4.1 Estimation of state vector dynamics . . . 13
  - 4.1.1 Estimation of risk-neutral factor dynamics . . . 13
  - 4.1.2 Estimation of data generating factor dynamics . . . 14
- 4.2 Estimation of inflation and risk-free rate parameters . . . 14

5 Empirical analysis **14**
- 5.1 Data . . . 14
- 5.2 Five-factor specification . . . 15
- 5.3 Six-factor specification . . . 18
  - 5.3.1 Inflation forecasting with the six-factor specification . . . 27
  - 5.3.2 Impact from the indexation lag . . . 28
- 5.4 IRF analysis of the six-factor specification . . . 29
  - 5.4.1 Level shock . . . 30
  - 5.4.2 Liquidity shock . . . 31
  - 5.4.3 Robustness to Cholesky ordering . . . 32

6 Discussion and conclusions **32**

1 Introduction

The expected path of inflation is an important macroeconomic variable that affects consumption, investment and policy decisions in the economy. Modern central banks conduct monetary policy on a mandate of long-term price stability, commonly defined as a tight interval around two percent. A key determinant of the path of inflation are long term inflation expectations since these affect, among other things, economic planning and investment decisions of firms and households and tend to feed into wages and price setting. Effective monetary policy therefore relies on maintaining well anchored aggregate inflation expectations in the economy and deviations from the inflation target are closely monitored by monetary policy makers. Among the most prevalent measures of inflation expectations are surveys of financial markets participants and households. Inflation expectations can also be gauged from the yields of government bonds at different maturities. Default-free nominal government bond yields represent real interest rates and the inflation compensation that investors demand. Hence, the shape of the yield curve contains information about the expected path of inflation. Fama (1990) and Mishkin (1990) for instance attempt to forecast inflation with nominal yield spreads.

Since 1994 the Swedish National Debt Office (SNDO) has issued inflation-linked government bonds (SGBi) alongside nominal government bonds (SGB). The cash flows from inflation-linked bonds are indexed to the Swedish consumer price index (CPI), meaning that they offer coupon and principal payments denominated in real terms. The yield spread between two matched maturity nominal and inflation-linked government bonds, called the breakeven inflation rate (BEI), is the average inflation rate that equalizes the return of the two bonds if held to maturity. For this reason, BEI is often viewed as a financial market measure of inflation expectations. Market based measures such as BEI are appealing since market efficiency implies that bond prices reflect unbiased inflation forecasts at available maturities. In addition, since BEI is observed at intra-daily frequency, it is readily available to policy makers, while surveys are published monthly or quarterly. The information in BEI is however distorted in two important ways. First, the inflation compensation that nominal bondholders receive is a combination of expected average inflation and inflation risk premia, which is the additional return demanded by investors for being exposed to inflation uncertainty. Second, the nominal government bond market, both in terms of debt outstanding and turnover, is many times larger than the inflation-indexed bond market. Search costs when trading SGBis are therefore higher and investors demand a liquidity premium for holding SGBis instead of SGBs. These relationships can be summarized in the following way:

$$
\begin{aligned}
y_t^{(m)} &= y_R^{(m)} + \rho_t^{(m)} + \mathbb{E}_t(\pi^{(m)}) + \mathrm{IRP}_t^{(m)}, \\
y_{\mathrm{IL},t}^{(m)} &= y_R^{(m)} + \rho_t^{(m)} + \mathrm{LP}_t^{(m)}, \\
\mathrm{BEI}_t^{(m)} &= y_t^{(m)} - y_{\mathrm{IL},t}^{(m)} = \mathbb{E}_t(\pi^{(m)}) + \mathrm{IRP}_t^{(m)} - \mathrm{LP}_t^{(m)},
\end{aligned}
$$

where $y_t^{(m)}$ and $y_{\mathrm{IL},t}^{(m)}$ are the yields at time t of a nominal and an inflation-linked zero-coupon bond with maturity in m periods. $y_R^{(m)}$ is the corresponding real yield and $\rho_t^{(m)}$ is the real interest rate risk premium. $\mathbb{E}_t(\pi^{(m)})$ is the average annual expected inflation rate from t to $t+m$. $\mathrm{IRP}_t^{(m)}$ is the inflation risk premium priced in the nominal bond while $\mathrm{LP}_t^{(m)}$ is

the liquidity premium priced in the inflation-linked bond. The sign of the bias to expected inflation in BEI at a given horizon depends on the relative size of the two distortions. To accurately describe BEI, one must also consider the time-varying nature of these premia.

We adopt an affine term structure model proposed in Abrahams et al. (2016) that jointly prices the nominal and inflation-linked term structures and estimate the expected inflation, inflation risk premium and liquidity premium components in Swedish breakeven inflation. The model allows us to add an observable liquidity factor, constructed from measures of bond market liquidity, to the set of pricing factors, which is used to identify time varying liquidity premia in inflation-linked bond yields. The model is estimated over the period 2006-2025 and the decomposition is performed on breakeven rates from 2-year to 10-year maturities. To the best of our knowledge, our study is among the first to estimate and decompose the term structure of Swedish breakeven inflation. The model is estimated on nominal and inflation-linked zero-coupon yield curves, which we estimate using the Nelson-Siegel-Svensson and Nelson-Siegel methods. The zero-coupon yield curve construction is detailed in Appendix A1. We review the related literature in section 2. The model is presented in section 3 followed by its estimation in 4. In the empirical analysis 5, we first present the results of a benchmark model using three nominal and two inflation-linked principal components as pricing factors 5.2. The results from our preferred specification, where we include the liquidity factor, are presented in section 5.3. The decomposition shows that BEI is a noisy measure of inflation expectations across all maturities, particularly during two periods of market stress: the global financial crisis 2008-2009 and the inflation shock in 2022-2023. Variation in risk premia explain most of the variation in BEI, with time varying inflation risk premia accounting for a dominant share of long term BEI variation. In 5.3.1 we compare the inflation forecasting ability of our estimated inflation expectation series to unadjusted BEI rates and survey forecasts. The model does not account for the three month indexation lag in Swedish inflation-linked bonds, the limitations of which are discussed in 5.3.2. We end the empirical analysis by studying the dynamic responses of each BEI component to structural shocks in short rates, proxied by the level factor, and liquidity shocks in section 5.4. We find that the dynamic response of BEI to level shocks transmit through inflation risk premia and inflation expectations. Liquidity shocks compress BEI almost entirely through the liquidity premium channel, with effects that are considerably more pronounced at shorter maturities. We discuss our main results and conclude in section 6.

2 Background and related literature

Structural models of the yield curve attempt to decompose bond yields into expected future short rates and compensation for exposure to systematic risk factors in an internally consistent way. In these models, bond prices are determined by a stochastic discount factor (SDF), driven by a set of pricing factors that describe how bond yields evolve over time. The expected path of the factors govern short rate expectations, and risk premia are driven by factor shocks. Arbitrage-free zero-coupon bond prices are then derived from the conditional expectations of future discount factors (see Cochrane (2005) for a primer). Functional form restrictions on the dynamics of the discount factor need to be imposed to make the models computationally feasible. Affine term structure models (ATSM) are frequently used in the literature and

assume that yields are linear in the vector of pricing factors (Duffie and Kan, 1996). Combined with a SDF that is log-linear in shocks to the state vector, this delivers closed form bond prices. Piazzesi (2010) provides an overview of affine models. Several studies document that bond risk premia are time varying with respect to the level of state variables, such as the slope of the yield curve (see for instance Fama and Bliss (1987) and Campbell and Shiller (1991)). The essentially affine specification of Duffee (2002) generates time varying risk premia by allowing the prices of factor risk to depend on the factor levels, independently of factor volatility. Discrete time adaptations of the ATSM framework are studied in for example Ang and Piazzesi (2003), Abrahams et al. (2016) and Adrian et al. (2013). In terms of factor structure, ATSMs can be based on latent factors (e.g. D'Amico et al. (2018) and Christensen et al. (2010)) or observable factors (e.g. Abrahams et al. (2016) and Adrian et al. (2013)) or a combination of the two (e.g. Ang and Piazzesi (2003)). Latent factor models, where the state variables are inferred from the yield data, tend to fit the term structure well but at the cost of producing factors that are not directly economically interpretable. With observable factor structures, factors from the yield cross-section and macroeconomic factors can be incorporated in a transparent way.

In arbitrage-free bond markets, the spread between nominal and real yields equals the expected average rate of inflation plus an inflation risk premium. In a consumption based asset pricing framework, this premium is determined by the covariance between the expected future real returns of nominal bonds and the investors' marginal utility of consumption, represented by the SDF. If inflation shocks are perceived to be associated with lower future consumption growth, then inflation risk premia will be positive and increase with bond maturity. If on the other hand inflation risk is perceived to hedge consumption risk, then the inflation risk premium can be negative (Piazzesi and Schneider, 2006). In a capital asset pricing model (CAPM) framework, the inflation risk premia in nominal bonds depend on the relationship between inflation shocks and equity returns. Campbell et al. (2009b) find that positive nominal bond risk premia in the 1980s and negative risk premia in the 2000s in the US were associated with the sign of the covariance between inflation shocks and equity returns going from negative to positive. In other words, stagflationary risk could be an important driver of inflation risk premia, while deflationary episodes are expected to suppress it. Obtaining a clean measure of the inflation risk premium directly from the yield spread between nominal and inflation-linked bonds is however complicated by the lagged indexation structure of inflation-linked bonds. Due to incomplete indexation, the bond holder is exposed to inflation risk the final months before the bond matures. For UK inflation-linked bonds where the indexation lag is 8 months, Evans (1998) finds evidence that the implied inflation risk premium present in inflation-linked bonds is small, around 1.5 basis points (bp), but statistically significant and time varying. Another influence on inflation-indexed yields in relation to real yields is the difference in liquidity between inflation-linked and nominal bonds. Campbell et al. (2009a) for instance document that the steep drop in US BEI during the financial crisis of 2008 was caused by a sudden rise in TIPS (Treasury inflation-protected securities) yields across all maturities, while Treasury yields remained stable. They attribute this to a large number of distressed sellers of TIPS following the collapse of Lehman Brothers for which there was limited demand as institutional investors and market makers were not willing or able to take positions in these securities. Pflueger and Viceira (2013) find that the liquidity risk premium in US

TIPS is time-varying, rising from 30 bp in 2005 to 150 bp in 2008-2009. They argue that liquidity risk is systematically priced in TIPS and relates to several market conditions such as the level of investor risk aversion, financing costs for arbitrageurs, and TIPS market search frictions. It is also plausible that the large share of outstanding inflation-linked debt held by institutional investors such as pension fund and insurance companies to hedge their real liabilities, as highlighted by Campbell et al. (2009a), suppresses inflation-linked bond turnover. For instance, Andreasen et al. (2020) find evidence that the liquidity premium is smaller for recently issued TIPS and attribute this to an increasing share of outstanding bond amounts entering buy-and-hold portfolios over time.

Several papers have jointly modeled the nominal and inflation-linked term structures to study the dynamics of BEI rates. Christensen et al. (2010) estimate a restricted ATSM with three nominal factors (level, slope and curvature) and one real level factor for US BEI, where the Nelson-Siegel (Nelson and Siegel, 1987) yield curve loading structure is imposed to facilitate estimation. Their estimated inflation expectations are stable around 2.4%, but the yield fit deteriorates during the financial crises which is partly attributed to the absence of liquidity risk in their model. Hördahl and Tristani (2012) incorporate macroeconomic factors in an ATSM to estimate inflation expectations and inflation risk premia in euro area BEI. In their results, 10-year expected inflation is well anchored around 2% and the 10-year average inflation risk premium is 20 bp. Their estimated inflation risk premium is counter cyclical and short term variations are negatively associated with changes in the output gap, consistent with stronger risk sentiment during economic expansions. D'Amico et al. (2018) specify an ATSM with a latent TIPS specific liquidity factor. Their estimated liquidity premium in TIPS yields exhibits large fluctuations. The 10-year TIPS liquidity premium fell from 150 bp when TIPS where introduced in 1997, to only a few basis points before the financial crisis, and then spiked at over 200 bp after the collapse of Lehman Brothers. The authors also document that similar to other studies, the US inflation risk premium trended downwards during the 2000s and in the early 2010s, consistent with a similar trend in inflation over the same period. Abrahams et al. (2016) specify an ATSM that jointly prices Treasury and TIPS yields with six observable factors and estimate inflation expectations, inflation risk premia and liquidity premia in US BEI 1999-2014. The estimated liquidity premium is identified from yield loadings on a composite liquidity index, constructed from two separate indicators of relative liquidity conditions in the TIPS market. While transparent, this approach relies on the accuracy of the liquidity data. Volatility in long-run BEI rates is found to be primarily driven by inflation risk and liquidity premia and the drop in BEI during the financial crisis is almost entirely explained by an elevated liquidity premium. In section 4, we estimate the components in Swedish BEI using the model in Abrahams et al. (2016). Contrary to D'Amico et al. (2018) and Abrahams et al. (2016), Andreasen et al. (2020) identify the liquidity premium from TIPS price differentials, accounting for the lower expected future liquidity of specific inflation-linked bonds as the share held in buy-and-hold portfolios tends to increase over time. Their estimated liquidity premium is similar to the estimates in Abrahams et al. (2016), averaging 25 bp for 10-year TIPS.

Considering that the Swedish government was an early issuer of inflation-linked bonds, surprisingly little research has been done on the informational content in Swedish BEI.

Although the Swedish government debt – especially traded debt following the Riksbanks's large scale asset purchase program in the mid 2010s and early 2020s – in recent decades has remained small by international comparison, the nominal government bond market is considered liquid and well functioning, in part due to SNDO's repo facility. The Swedish inflation-linked bond market is however thin which complicates studies like ours where multiple bond yields must be observed in the cross section to estimate the term structure reliably. In our data set, the median number of outstanding inflation-linked bonds per observation date between 2000 and 2025 was 6, while the median number of outstanding nominal bonds was 11. In Appendix A1, we detail our estimation of zero-coupon yield curves for Swedish inflation-linked bonds using the Nelson-Siegel method. Alexandersson (2018) estimates the liquidity premium in Swedish 5-year forward BEI by regressing BEI on observable liquidity proxies, controlling for proxies of expected inflation and inflation risk. Similar to the results in Pflueger and Viceira (2013) on US BEI, the regression R^2 increases from 35% to 68% when four different liquidity proxies are included. This indicates that liquidity conditions have a meaningful impact on Swedish BEI. Recent communication from the SNDO also suggests that inflation-linked bond market illiquidity will become even more pronounced in the years to come. In September 2024 the SNDO announced that they aim to reduce the amount of outstanding inflation-linked debt from 177 billion SEK, which was roughly 20% of total debt at the time, to 80 billion SEK by the end of 2029[1]. In the announcement, the SNDO specifically cited the liquidity premium – which raises their borrowing cost – as a cost disadvantage that informed their decision. In light of higher nominal bond issuance[2], a plausible consequence is that the liquidity distortions in Swedish breakeven rates will grow. For monetary policy makers and financial market participants who use BEI to assess inflation expectations, it therefore becomes extra important to understand the current magnitude and behavior of the liquidity premium. In section 5.3 we present the results of our decomposition of Swedish BEI at different horizons.

3 A joint nominal and inflation-linked no-arbitrage affine term structure model

According to asset pricing theory, in the absence of arbitrage opportunities, long maturity interest rates are risk-adjusted expectations of average future short interest rates. By the assumption of no-arbitrage, there exists a one-period stochastic discount factor M_{t+1} that prices all next period payoffs in the economy. The price of a one-period zero-coupon bond with SEK 1 face value is determined by the conditional expectation of the next-period discount factor: $P_t^{(1)} = E_t[M_{t+1} \cdot 1]$. Extending this logic over several periods, the price of a m-period zero-coupon bond equals the conditional expectation of the product of all one-period discount factors until maturity:

$$P_t^{(m)} = E_t\left[M_{t+1} \cdot P_{t+1}^{(m-1)}\right] = E_t[M_{t+1} \cdot M_{t+2} \cdot ... \cdot M_{t+m}]\,.$$

[1] Riksgälden (2024), *Statsskuldens förvaltning – Förslag till riktlinjer 2025–2027*, Dnr 2024/388.

[2] The SNDO plans to increase annual nominal bond issuance from 118 billion SEK in 2025 to 220 billion SEK in 2027 as the total government debt is expected to increase by 38%. Riksgälden (2025), *Statsupplåning – Prognos och analys 2025:2*, Dnr 2025/347.

No-arbitrage term structure models assume that the discount factor is dependent on the evolution of a set of state variables that describe the behavior of bond yields. Arbitrage-free zero-coupon bond prices are given by the conditional expectation of the discount factor. The class of affine term structure models assume that bond prices are exponentially affine in the state vector: $\log P_t^{(m)} = A_m + B_m' X_t$, where no-arbitrage is imposed through cross-equation restrictions on the pricing coefficients A_m and B_m. Abrahams et al. (2016) specify an ATSM where a $K \times 1$ vector of pricing factors is assumed to follow a discrete Gaussian VAR(1) process

$$X_{t+1} - \mu_x = \Phi(X_t - \mu_x) + v_{t+1}. \tag{1}$$

The vector of factor shocks v_{t+1} is assumed to be normally distributed with $E_t(v_{t+1}) = \mathbf{0}$ and $E_t(v_{t+1} v_{t+1}') = \Sigma_{K \times K}$. The off-diagonal elements σ_{ij} in the covariance matrix are the factor shock covariances, while diagonal elements σ_{ii} are the shock variances. The transition matrix Φ governs the dynamics of the state vector. Diagonal elements ϕ_{ii} determine factor persistence and ϕ_{ij} determine spillover effects between factors. The long run mean of the system is governed by μ_x. The one-period continuously compounded risk-free rate in the economy, denoted r, is assumed to be an affine function of the pricing factors. The one-period SDF is assumed to be exponentially affine in the factor shocks which implies that its distribution is conditionally log-normal.

$$r_t = \delta_0 + \delta_1' X_t \tag{2}$$

$$M_{t+1} = \exp\Big(- r_t - \frac{1}{2} \lambda_t' \lambda_t - \lambda_t' \Sigma^{-\frac{1}{2}} v_{t+1} \Big) \tag{3}$$

The first term in the SDF discounts at the risk-free rate and the second term is a convexity correction which ensures that one-period bonds are priced correctly: $E_t(M_{t+1}) = e^{-r_t} = P_t^{(1)}$. Risk premia are generated from the response of the SDF to standardized factor shocks, $\Sigma^{-\frac{1}{2}} v_{t+1} \sim \mathcal{N}(0, I)$, which is governed by a $K \times 1$ market price of risk vector λ_t. The price of risk vector follows the essentially affine form of Duffee (2002)

$$\lambda_t = \Sigma^{-\frac{1}{2}} \Big(\lambda_0 + \lambda_1 X_t \Big). \tag{4}$$

Because factor volatility is assumed constant, time varying risk premia are generated solely from changes in the state dependent market prices of risk through λ_1. λ_0 contains baseline prices of factor risk.

3.1 Risk neutral no-arbitrage bond pricing

By the assumption of no-arbitrage and the existence of a stochastic discount factor, there exists an alternative risk neutral probability measure $\mathbb{Q}$ under which the expected one-period bond of any bond equals the risk-free rate. Thus, under risk neutral probabilities, bond prices are discounted at the risk-free rate, which is convenient, and is equivalent to pricing under the data generating probability measure $\mathbb{P}$: $P_t^{(m)} = E_t^{\mathbb{P}}\Big[M_{t+1} \cdot P_{t+1}^{(m-1)} \Big] = E_t^{\mathbb{Q}}\Big[\exp(-r_t) \cdot P_{t+1}^{(m-1)} \Big]$. It can be shown that the probability of a state being realized under $\mathbb{Q}$ is the probability under $\mathbb{P}$, tilted by a factor $\exp(r_t) M_{t+1} = \exp\Big(- \frac{1}{2} \lambda_t' \lambda_t - \lambda_t' \Sigma^{-\frac{1}{2}} v_{t+1} \Big)$. By changing measures, the risk adjustment is handled by tilting the distribution of the shock vector so that it

obtains a new mean $E_t^{\mathbb{Q}}[v_{t+1}] = -\Sigma^{\frac{1}{2}}\lambda_t = -(\lambda_0 + \lambda_1 X_t)$[3]. Define a re-centered shock vector $v_{t+1}^{\mathbb{Q}} = v_{t+1} + (\lambda_0 + \lambda_1 X_t) \sim \mathcal{N}(0, \Sigma)$ and substitute into the state vector dynamics:

$$X_{t+1} = \mu_x + \Phi(X_t - \mu_x) + \left(v_{t+1}^{\mathbb{Q}} - \Big(\lambda_0 + \lambda_1 X_t\Big)\right),$$

$$X_{t+1} = \widetilde{\mu} + \widetilde{\Phi} X_t + v_{t+1}^{\mathbb{Q}}, \tag{5}$$

where $\widetilde{\mu} = (I - \Phi)\mu_x - \lambda_0$ and $\widetilde{\Phi} = (\Phi - \lambda_1)$ (Abrahams et al., 2016). The state vector process remains a Gaussian VAR(1) under the risk neutral measure, but with altered dynamics. The mean shifts through the baseline prices of factor risk λ_0 and λ_1 directly alters the factor persistence where factors with positive risk loadings ($\lambda_{1,ii} > 0$) for instance mean revert faster than they do under $\mathbb{P}$. The no-arbitrage condition under $\mathbb{Q}$ is

$$P_t^{(m)} = E_t^{\mathbb{Q}}\left[\exp\Big(-\sum_{i=0}^{m-1} r_{t+i}\Big)\right] \Leftrightarrow P_t^{(m)} = E_t^{\mathbb{Q}}\left[\exp(-r_t)P_{t+1}^{(m-1)}\right]. \tag{6}$$

We assume that the log price of a m-period bond is affine in the pricing factors: $\log P_t^{(m)} = A_m + B_m' X_t$, where A_m is a scalar and B_m is a $K \times 1$ vector. Since $P_t^{(0)} = 1$ it must be the case that $A_0 = 0$ and $B_0 = \mathbf{0}$. Furthermore, from equation (2) we know that $A_1 = -\delta_0$ and $B_1 = -\delta_1$. Substitute the expression for the log price together with (2) and (5) into the no-arbitrage condition in (6):

$$\log P_t^{(m)} = \log E_t^{\mathbb{Q}}\left[\exp(-\delta_0 - \delta_1' X_t)\exp\Big(A_{m-1} + B_{m-1}'(\widetilde{\mu} + \widetilde{\Phi} X_t + v_{t+1}^{\mathbb{Q}})\Big)\right],$$

$$\log P_t^{(m)} = -\delta_0 + A_{m-1} + B_{m-1}'\widetilde{\mu} + \Big(B_{m-1}'\widetilde{\Phi} - \delta_1'\Big)X_t + \log E_t^{\mathbb{Q}}\left[\exp\Big(B_{m-1}' v_{t+1}^{\mathbb{Q}}\Big)\right],$$

where $B_{m-1}' v_{t+1}^{\mathbb{Q}} \sim \mathcal{N}(0, B_{m-1}'\Sigma B_{m-1})$. Compute the conditional expectation, $E_t^{\mathbb{Q}}\left[\exp\Big(B_{m-1}' v_{t+1}^{\mathbb{Q}}\Big)\right] = \exp\Big(\frac{1}{2}B_{m-1}'\Sigma B_{m-1}\Big)$, and collect terms to obtain the log price coefficients at maturity m (Abrahams et al., 2016):

$$\log P_t^{(m)} = -\delta_0 + A_{m-1} + B_{m-1}'\widetilde{\mu} + \frac{1}{2}B_{m-1}'\Sigma B_{m-1} + \Big(B_{m-1}'\widetilde{\Phi} - \delta_1'\Big)X_t,$$

$$A_m = A_{m-1} + B_{m-1}'\widetilde{\mu} + \frac{1}{2}B_{m-1}'\Sigma B_{m-1} - \delta_0, \quad B_m' = B_{m-1}'\widetilde{\Phi} - \delta_1'. \tag{7}$$

By recursively applying the coefficient expressions in (7), given initial values $A_0 = 0$ and $B_0 = \mathbf{0}$, we obtain the closed form coefficient expressions:

$$A_m = -m\delta_0 + \sum_{i=0}^{m-1}\Big(B_i'\widetilde{\mu} + \frac{1}{2}B_i'\Sigma B_i\Big), \quad B_m' = -\delta_1'\sum_{i=0}^{m-1}\widetilde{\Phi}^i. \tag{8}$$

From the closed form expressions, we can see that B_m' determines how current conditions X_t are expected to propagate through the risk neutral dynamics to influence each future short rate up to maturity. Persistent factors will therefore cause long maturity yields to respond

[3] Piazzesi (2010) provides a technical treatment in continuous time. For a more detailed treatment in discrete time, see e.g. Ang and Piazzesi (2003).

strongly to changes to current conditions. A_m collects all constant, state independent terms. These include the state independent component of expected future short rates under the risk neutral measure, as well as the convexity corrections that arise because bond prices are exponentially affine in state. The exponential affine form of bond prices imply that bond yields are affine in the pricing factors

$$y_t^{(m)} = -\frac{1}{m}\log P_t^{(m)} = -\frac{1}{m}\Big(A_m + B_m' X_t\Big). \tag{9}$$

3.2 Real bonds

Real bonds are effectively nominal bonds whose cash flows are perfectly indexed to CPI. Abrahams et al. (2016) treat inflation-linked bonds as real bonds and assume that real and nominal bond log prices are affine functions of the same set of pricing factors. Let Q_t denote the CPI at time t. The price of a real zero-coupon bond with SEK 1 face value is given by:

$$P_{t,R}^{(m)} = E_t^{\mathbb{Q}}\left[\exp\Big(-\sum_{k=0}^{m-1} r_{t+k}\Big)\frac{Q_{t+m}}{Q_t}\right].$$

Denote one-period log inflation rate as $\pi_{t+1} = \ln Q_{t+1}/Q_t$. The no-arbitrage condition for inflation-linked bonds becomes

$$P_{t,R}^{(m)} = E_t^{\mathbb{Q}}\left[\exp\Big(\sum_{i=0}^{m-1} -r_{t+i} + \pi_{t+i+1}\Big)\right] \Leftrightarrow P_{t,R}^{(m)} = E_t^{\mathbb{Q}}\Big[\exp(-r_t + \pi_{t+1})P_{t+1,R}^{(m-1)}\Big]. \tag{10}$$

For the pricing recursions to generate exponentially affine prices for real bonds, the one period log inflation rate must also be affine in the pricing factors

$$\pi_t = \pi_0 + \pi_1' X_t. \tag{11}$$

Substitute the log price form $\log P_{t,R}^{(m)} = A_{m,R} + B_{m,R}' X_t$ together with (2), (5) and (11) into the no-arbitrage condition (10):

$$\log P_{t,R}^{(m)} = \log E_t^{\mathbb{Q}}\Big[\exp\Big(-\delta_{0,R} - \delta_1' X_t\Big)\exp\Big(A_{m-1,R} + \widetilde{B}_{m-1,R}'(\widetilde{\mu} + \widetilde{\Phi} X_t + v_{t+1}^{\mathbb{Q}})\Big)\Big],$$

$$\log P_{t,R}^{(m)} = -\delta_{0,R} + A_{m-1,R} + \widetilde{B}_{m-1,R}'\widetilde{\mu} + \Big(\widetilde{B}_{m-1,R}'\widetilde{\Phi} - \delta_1'\Big)X_t + \log E_t^{\mathbb{Q}}\Big[\exp\Big(\widetilde{B}_{m-1,R}' v_{t+1}^{\mathbb{Q}}\Big)\Big],$$

where $\widetilde{B}_{m-1,R}' = (\pi_1 + B_{m-1,R})'$ and $\delta_{0,R} = \delta_0 - \pi_0$. Compute the conditional expectation and collect terms to obtain the real coefficient expressions:

$$\log P_{t,R}^{(m)} = -\delta_{0,R} + A_{m-1,R} + \widetilde{B}_{m-1,R}'\widetilde{\mu} + \frac{1}{2}\widetilde{B}_{m-1,R}'\Sigma\widetilde{B}_{m-1,R} + \Big(\widetilde{B}_{m-1,R}'\widetilde{\Phi} - \delta_1'\Big)X_t,$$

$$A_{m,R} = A_{m-1,R} + \widetilde{B}_{m-1,R}'\widetilde{\mu} + \frac{1}{2}\widetilde{B}_{m-1,R}'\Sigma\widetilde{B}_{m-1,R} - \delta_{0,R}, \quad B_{m,R} = \widetilde{B}_{m-1,R}'\widetilde{\Phi} - \delta_1'. \tag{12}$$

Since $P_{t,R}^{(0)} = 1 \cdot \frac{Q_t}{Q_t} = 1$ it must be the case that $A_{0,R} = 0$ and $B_{0,R} = \mathbf{0}$. The closed form coefficient expressions are given by:

$$A_{m,R} = -m\delta_{0,R} + \sum_{i=0}^{m-1}\Big(\widetilde{B}_{i,R}'\widetilde{\mu} + \frac{1}{2}\widetilde{B}_{i,R}'\Sigma\widetilde{B}_{i,R}\Big), \quad B_{m,R} = -\delta_1'\sum_{i=0}^{m-1}\widetilde{\Phi}^i + \pi_1'\sum_{j=1}^{m}\widetilde{\Phi}^j. \tag{13}$$

Real yields depend on the expected paths of the short rate and inflation, and $B_{m,R}$ therefore also considers how current conditions are expected to influence future inflation. Similarly, $A_{m,R}$ is the counterpart to A_m with convexity corrections that additionally account for inflation uncertainty. It follows that real bond yield are:

$$y_{t,R}^{(m)} = -\frac{1}{m}\Big(A_{m,R} + B'_{m,R}X_t\Big). \tag{14}$$

3.3 Break-even inflation decomposition

Arbitrage-free zero-coupon BEI rates are defined as the difference between nominal yields (9) and real yields (14):

$$\text{BEI}_t^{(m)} = y_t^{(m)} - y_{t,R}^{(m)} = -\frac{1}{m}\big[(A_m - A_{m,R}) + (B_m - B_{m,R})'X_t\big]. \tag{15}$$

The risk neutral pricing recursions in sections 3.1 and 3.2 embed compensation for all priced factor risks through the distorted state vector dynamics in equation (5). Since nominal prices are discounted at the risk free rate, and inflation-linked prices are discounted at the real risk-free rate, BEI equals the risk neutral expectation of average future inflation rates. Therefore, if we perform the same recursions using the actual state vector dynamics, the implied BEI will reflect actual inflation expectations. We do this by replacing the risk neutral parameters $\{\widetilde{\mu}, \widetilde{\Phi}\}$ for the actual parameters $\{(I-\Phi)\mu_x, \Phi\}$ in the pricing recursions (7) and (12). The difference between the new $\mathbb{P}$-measure nominal and real yields is the model implied m-period expected average inflation:

$$E_t(\pi^{(m)}) = -\frac{1}{m}\big[(A_m^{\mathbb{P}} - A_{m,R}^{\mathbb{P}}) + (B_m^{\mathbb{P}} - B_{m,R}^{\mathbb{P}})'X_t\big]. \tag{16}$$

The difference between BEI (15) and expected inflation (16) constitutes the total risk premium in BEI. We follow Abrahams et al. (2016) and assume that the total risk premium has two components: an inflation risk premium and a liquidity risk premium. Other risk premia, such as the real interest rate risk premium, appear in both nominal and real bonds and are therefore differenced out in BEI. Because nominal bonds are exposed to inflation risk while real bonds are not, the inflation risk premium contributes positively to BEI. As discussed in section 2, investors may also demand a liquidity premium for holding inflation-linked bonds instead of nominal bonds which contributes negatively to BEI. The model structure allows us to include an observed liquidity factor $\mathcal{L}_t$ in the state vector. The time-varying contribution of the liquidity factor to nominal and real yields is $-\frac{1}{m}b_m^{(\mathcal{L})}\mathcal{L}_t$ and $-\frac{1}{m}b_{m,R}^{(\mathcal{L})}\mathcal{L}_t$ respectively, where $b_m^{(\mathcal{L})}$ and $b_{m,R}^{(\mathcal{L})}$ are the elements in B_m and $B_{m,R}$ corresponding to $\mathcal{L}$. Liquidity adjusted expected inflation and inflation risk premia are constructed by subtracting time varying liquidity contributions from nominal and real yields before computing equation (16). The time varying liquidity contribution to BEI is equal to the difference between actual and liquidity adjusted BEI.

$$\text{BEI}_t^{(m),adj} = y_t^{(m),adj} - y_{t,R}^{(m),adj} = -\frac{1}{m}\big[(A_m - A_{m,R}) + (B_m^{(-\mathcal{L})} - B_{m,R}^{(-\mathcal{L})})'X_t^{(-\mathcal{L})}\big],$$

$$E_t(\pi^{(m)})^{adj} = -\frac{1}{m}\big[(A_m^{\mathbb{P}} - A_{m,R}^{\mathbb{P}}) + (B_m^{\mathbb{P},(-\mathcal{L})} - B_{m,R}^{\mathbb{P},(-\mathcal{L})})'X_t^{(-\mathcal{L})}\big],$$

$$\mathrm{IRP}^{(m),adj} = \mathrm{BEI}_t^{(m),adj} - E_t(\pi^{(m)})^{adj},$$

$$\underbrace{\mathrm{BEI}_t^{(m)}}_{\text{break-even inflation}} = \underbrace{E_t(\pi^{(m)})^{adj}}_{\text{adjusted inflation expectations}} + \underbrace{\mathrm{IRP}_t^{(m),adj}}_{\text{adjusted inflation risk premium}} + \underbrace{\mathrm{LP}_t^{(m)}}_{\text{liquidity premium}}.$$

3.4 Inflation-linked bonds

Inflation-linked bonds are different from real bonds in that their cash flows are not perfectly indexed to CPI. While a real bondholder receives inflation compensation that matches the bond's term to maturity from t to $t+m$, inflation-linked bonds are indexed with a l-period lag, i.e. from $t-l$ to $t+m-l$. For SGBis, the indexation lag is three months. The price of a m-period inflation-linked zero-coupon bond with face value SEK 1 is therefore:

$$P_{t,IL}^{(m)} = E_t^{\mathbb{Q}}\left[\exp\Big(-\sum_{k=0}^{m-1} r_{t+k}\Big)\frac{Q_{t+m-l}}{Q_{t-l}}\right] = \frac{Q_t}{Q_{t-l}}E_t^{\mathbb{Q}}\left[\exp\Big(-\sum_{k=0}^{m-1} r_{t+k}\Big)\frac{Q_{t+m-l}}{Q_t}\right],$$

where we use the fact that the CPI from $t-l$ to t is known. This means that the return of an inflation-linked bond contains a deterministic inflation component, equal to the log inflation already accrued at t. We refer to this deterministic component as the carry which in annualized terms lowers inflation-linked bond yields by an amount $\frac{12}{m}\ln Q_t/Q_{t-l} = \frac{12}{m}\sum_{i=0}^{l-1}\pi_{t-i}$. Abrahams et al. (2016) do not account for the effect of the indexation lag and treat inflation-linked bonds as if they where real. In sections 5.2 and 5.3, we estimate the model ignoring the indexation lag. If realized inflation from $t-l$ to t however does not match the inflation expectations for the periods $t+m-l$ to $t+m$, the carry will bias inflation-linked yields downwards compared to real yields, overstating the forward looking content in BEI. Since the model does not separately identify this distortion, it will be absorbed into the estimated BEI decomposition. This bias is potentially sizable during the post-covid inflationary shock which is included in our sample.

4 Parameter estimation

The joint ATSM presented in section 3 establishes that real and nominal yields are affine functions of the set of pricing factors X_t. The closed form coefficient expressions reveal that (A_m, B_m) and $(A_{m,R}, B_{m,R})$ are pinned down by the parameters $\{\mu, \Phi, \Sigma, \widetilde{\mu}, \widetilde{\Phi}, \delta_0, \delta_1, \pi_0, \pi_1\}$ which must be estimated from observed yields, where the price of risk parameters $\{\lambda_0, \lambda_1\}$ correspond to the wedge between $\{\mu, \Phi\}$ and $\{\widetilde{\mu}, \widetilde{\Phi}\}$. Estimation is conducted following the Abrahams et al. (2016) adaptation of the three step linear regression based estimation procedure for affine term structure models proposed in Adrian et al. (2013), which exploits the fact that excess holding period returns are linear in $\widetilde{\Phi}$. First, the dynamics of the state vector are estimated from a time series regression. Second, excess return loadings of contemporary and lagged values of the pricing factors are estimated by ordinary least squares (OLS). In a third step, $\hat{\widetilde{\mu}}$ and $\hat{\widetilde{\Phi}}$ are recovered from the regression coefficient and intercept in the second step by generalized least squares (GLS). The short-rate parameters are estimated from a time series regression. Because real bond returns are quadratic in the parameter π_1, $\hat{\pi}_0$ and $\hat{\pi}_1$ are finally obtained from numerically minimizing the sum of squared excess return fitting errors.

4.1 Estimation of state vector dynamics

The one period holding return on a nominal bond in excess of the the risk free return is defined by $rx_{t+1}^{(m)} = \log P_{t+1}^{(m-1)} - \log P_t^{(m)} - r_t$. Similarly, the excess holding period return of a real bond, including the realized inflation compensation, is $rx_{t+1,R}^{(m)} + \pi_{t+1} = \log P_{t+1,R}^{(m-1)} - \log P_{t,R}^{(m)} - r_t + \pi_{t+1}$. Substituting the affine expressions of log prices and the recursive coefficient expressions (7) and (12) we get:

$$rx_{t+1}^{(m)} = \alpha_{m-1} - B_{m-1}'\tilde{\Phi}X_t + B_{m-1}'X_{t+1} \tag{17}$$

$$rx_{t+1,R}^{(m)} + \pi_{t+1} = \alpha_{m-1,R} - (B_{m-1,R} + \pi_1)'\tilde{\Phi}X_t + (B_{m-1,R} + \pi_1)'X_{t+1} \tag{18}$$

where $\alpha_{m-1} = -\left(B_{m-1}'\tilde{\mu} + \frac{1}{2}B_{m-1}'\Sigma B_{m-1}\right)$ and $\alpha_{m-1,R} = -\Big(\pi_0 + (B_{m-1,R}+\pi_1)'\tilde{\mu} + \frac{1}{2}(B_{m-1,R} + \pi_1)'\Sigma(B_{m-1,R} + \pi_1)\Big)$ are maturity specific intercepts. Nominal and real excess returns depend linearly on current and lagged levels of the pricing factors. Stacking all N_N nominal and N_R real excess returns into one return vector R_{t+1}^{π} and defining $B_{N\times K} = (B_1, \ldots, B_{N_N}, B_{1,R} + \pi_1, \ldots, B_{N_R,R} + \pi_1)'$, we obtain a joint return vector which is linear in the factors:

$$R_{t+1}^{\pi} = \alpha - B\tilde{\Phi}X_t + BX_{t+1} + E_{t+1} \tag{19}$$

where $\alpha_{N\times 1} = -(B\tilde{\mu} + \frac{1}{2}\gamma)$ and γ collects the cross sectional convexity correction terms. E_{t+1} collects cross sectional return errors. Identification by OLS requires that the return errors have zero conditional mean and constant covariance Σ_e. It is further assumed that the return errors are serially uncorrelated, implying that the only source of predictability in excess returns is generated by the pricing factors. Stacking the return vectors (19) across all T periods in the sample, we get a $N \times T$ return system:

$$R_{N\times T} = \alpha\iota' - B\tilde{\Phi}X_{_} + BX + E \tag{20}$$

where ι is a $T \times 1$ vector of ones. The stacked system is estimated row by row (by maturity) with OLS to obtain $\hat{\alpha}_{\text{ols}}$, $\widehat{B\tilde{\Phi}}_{\text{ols}}$ and $\hat{B}_{\text{ols}}$, along with a consistent estimator of the return error covariance $\hat{\Sigma}_e = T^{-1}\hat{E}\hat{E}'$.

4.1.1 Estimation of risk-neutral factor dynamics

The estimated $N \times K$ matrices $\widehat{B\tilde{\Phi}}_{\text{ols}}$ are used to estimate the $K \times K$ risk-neural transition matrix $\tilde{\Phi}$. To account for the return correlations across maturities, the estimation is performed by GLS where each equation is weighted by the inverse of its error covariance in $\hat{\Sigma}_e$. The GLS estimator of $\tilde{\Phi}$ is

$$\hat{\tilde{\Phi}}_{\text{gls}} = \left(\hat{B}_{\text{ols}}'\hat{\Sigma}_e^{-1}\hat{B}_{\text{ols}}\right)^{-1}\hat{B}_{\text{ols}}'\hat{\Sigma}_e^{-1}\widehat{B\tilde{\Phi}}_{\text{ols}}. \tag{21}$$

Because bond returns across adjacent maturities are highly correlated, we find that some maturities in the return space are poorly identified in our data which makes $\hat{\Sigma}_e$ near-singular. Taking the inverse of the near singular covariance matrix caused $\hat{\tilde{\Phi}}$ to become non-stationary and bond prices to diverge in the pricing recursions. We handle this by computing a pseudo-inverse of $\hat{\Sigma}_e$, zeroing out singular values below a threshold relative to the largest singular value before inverting the matrix. This effectively preserves only the information from the well-identified return equations.

More efficient estimates of B and α are obtained by re-specifying the return vector in (19) as $R_{t+1} = \alpha + B(X_{t+1} - \hat{\tilde{\Phi}}_{gls} X_t) + E_{t+1}$ and re-estimating the stacked return system. The GLS estimator for $\tilde{\mu}$ becomes

$$\hat{\tilde{\mu}}_{\text{gls}} = -\left(\hat{B}'_{\text{gls}} \hat{\Sigma}_e^{-1} \hat{B}_{\text{gls}}\right)^{-1} \hat{B}'_{\text{gls}} \hat{\Sigma}_e^{-1} \left(\hat{\alpha}_{\text{gls}} + \tfrac{1}{2}\hat{\gamma}_{\text{gls}}\right). \tag{22}$$

4.1.2 Estimation of data generating factor dynamics

The parameters Φ, μ are estimated by OLS from the demeaned factor process specified in equation (1). From the VAR residuals $\hat{v}_t$ we obtain a consistent estimator of the covariance matrix $\hat{\Sigma} = \frac{1}{T-1} \sum_{t=2}^{T} \hat{v}_t \hat{v}_t{}'$.

4.2 Estimation of inflation and risk-free rate parameters

Because the model is specified at monthly frequency, we use the observed one-month continuously compounded zero-coupon rate as the risk-free rate in the estimation. The risk-free rate parameters δ_0 and δ_1 are estimated by OLS according to equation (2). Inflation however, while observed, compounds in the real pricing recursions (13) through π_1. Abrahams et al. (2016) show that real bond yields and returns are quadratic in π_1 and linear in π_0. The non-linear relationship between returns and inflation is estimated by numerically minimizing the sum of squared errors between observed and model implied real excess returns, holding all previously estimated parameters fixed:

$$\{\hat{\pi}_0, \hat{\pi}_1\} = \arg\min_{\pi_0,\pi_1} \sum_{i=1}^{N_R} \sum_{t=1}^{T} \left(rx_{t+1,R}^{(m_i)} - \widehat{rx}_{t+1,R}^{(m_i)}(\pi_0, \pi_1; \hat{\tilde{\Phi}}, \hat{\tilde{\mu}}, \hat{\delta}_0, \hat{\delta}_1, \hat{\Sigma}) \right)^2, \tag{23}$$

where $\widehat{rx}_{t+1,R}^{(m_i)}(\cdot)$ denotes the model-implied real excess return at maturity m_i evaluated at the trial values of the inflation parameters. We use the OLS estimates from regressing the parameters on the state vector in equation (11) as initial values. To reduce the risk of convergence to a local optimum, the minimization is performed with search bounds centered on the OLS estimates. Specifically, π_0 is constrained within $\pm 2\%$ in annual terms of $\pi_{0,ols}$ and each element of π_1 is bounded within a multiple of its OLS magnitude.

5 Empirical analysis

In this section we present the results from two different model specifications. First, a five-factor model based on three principal components from nominal yields and two orthogonal principal components from inflation-linked yields is estimated to serve as a benchmark. In the six-factor specification, a composite liquidity index is included as a factor to enable decomposition of BEI into estimates of inflation expectations, inflation risk premia and liquidity premia.

5.1 Data

The model is estimated from a panel of nominal and inflation-linked zero-coupon yields. Default-free zero-coupon yields are not directly observable in bond markets but can be

inferred from the prices of traded coupon bonds. Still, there are a limited number of SGBs and SGBis traded at any point in time, so the zero-coupon yield curves must be estimated. We collect end-of-month prices from 2000-2025 on all traded SGBs and SGBis with available data in Bloomberg. Monthly nominal and inflation-linked yield curves are estimated using the parametric Nelson–Siegel–Svensson and Nelson–Siegel methods respectively, spanning from January 2006 to December 2025 for a total of $T = 240$ monthly observations. Estimation begins in 2006 as we deem the number of outstanding SGBis prior to this date insufficient to reliably identify the term structure across the maturities required. To mitigate the risk that the yield curve parameters are poorly identified, we add an artificial bond at the mid-point between each pair of adjacent bonds, constructed a smooth bootstrapped yield curve using the cubic spline interpolation method. The estimation is described in detail in Appendix A1. To estimate the model, we use nominal zero-coupon yields with $m = 6, 12, 24, \ldots, 120$ month maturities and inflation-linked zero-coupon yields at $m = 24, 36, \ldots, 120$ months. Consistent with Abrahams et al. (2016), the shortest inflation-linked maturity is set at 24 months to limit distortions from the indexation-lag. The risk-free rate used is the estimated one month nominal zero-coupon yield. Monthly inflation is measured as the log change in the CPI series with base year 1980 published by Statistics Sweden (SCB).

5.2 Five-factor specification

We begin by estimating the model using only principal components of nominal and inflation-linked zero-coupon yields as factors. The first three principal components (PC) are typically sufficient to explain almost all variation in yields and are commonly referred to as level, slope and curvature (Litterman and Scheinkman, 1991). The first three PCs from nominal yields, standardized to have zero mean and unit variance, are plotted in Figure 14. The first PC behaves like a level factor with roughly constant loadings across maturities and evolves in a similar pattern as the Riksbank's policy rate over time. The loadings on the second PC increase with maturity, consistent with a slope factor, while the loadings on the third PC peak at 2–4 year maturities, consistent with a curvature factor. According to a variance decomposition, the first, second and third PCs respectively explain 94.7%, 5.0% and 0.3% of nominal yield variation. SGBi and SGB yields are highly correlated. A regression of inflation-linked yields on the three nominal PCs generate an R^2 of 92.2%. To mitigate factor collinearity while still capturing unique inflation-linked yield variation, we follow Abrahams et al. (2016) and include two PCs from inflation-linked yields that are orthogonal to the nominal PCs. These are constructed from the residuals of regressing the inflation-linked zero-coupon yields on the three nominal PCs. The orthogonal inflation-linked PCs together explain 99.5% of the residual variance in inflation-linked yields. As is illustrated in figure 15, these also behave like a level and a slope factor.

The joint ATSM described in sections 3 and 4 is estimated with five pricing factors: three nominal PCs and two orthogonal inflation-linked PCs. Yield fit diagnostics are reported in table 7 and illustrated in figure 16. The model fits both yield curves well. The root mean squared nominal yield fitting error (RMSE) is 4.54 bp across all maturities and ranges from 3.28 bp at the 4-year maturity to 6.11 bp at the 10-year maturity. The inflation-linked fitting error across all maturities is 5.19 bp (RMSE), and is highest at the 2-year maturity with 8.83

bp RMSE. The yield pricing errors display high first-order autocorrelations ranging from 0.76 to 0.92 and meaningful sixth-order autocorrelations. This persistence is standard in affine term structure models and reflects the slow-moving nature of the yield curve: most often, bonds trade under similar conditions from one month to the next, causing pricing errors to persist. Excess return errors tell a different story. Return errors show near-zero autocorrelation at both lags across all maturities, with first-order autocorrelations between -0.19 and $+0.05$ for nominal bonds and between -0.12 and -0.01 for inflation-linked bonds. This asymmetry is a key diagnostic. Since excess return predictability is driven by time-varying risk premia, a well specified model should leave no predictable pattern in the residuals. Return errors are larger in magnitude as expected given the higher volatility of monthly holding returns and the yield specific pricing factors, with RMSE ranging from 7 bp for 2-year nominal bonds to 38 bp for 10-year for nominal bonds, and from 8 bp to 31 bp for inflation-linked bonds.

	Variance shares			Correlations		
Maturity	EI	IRP	Cov	$\rho(EI, IRP)$	$\rho(EI, BEI)$	$\rho(IRP, BEI)$
2Y	0.293	0.615	0.092	0.108	0.627	0.843
5Y	0.104	0.885	0.012	0.019	0.340	0.947
10Y	0.053	0.872	0.075	0.175	0.393	0.974

Table 1: **BEI variance decomposition and correlations, five-factor specification.** *Left:* Share of BEI sample variance explained by expected inflation (EI), the total risk premium (IRP), and the covariance component (Cov) at 2-, 5-, and 10-year horizons in decimals. *Right:* Sample correlations between estimated expected inflation, total risk premium, and BEI. *Source: Authors' calculations based on Bloomberg and Statistics Sweden (SCB) data (2006–2025).*

Table 4 contains summary statistics for the estimated BEI and its decomposition into expected inflation and total risk premium for the 5-factor model. Expected inflation averages around 1.33% at 2-year, 5-year and 10-year horizons, well below the 2% inflation target. The total risk premium is on average positive and increases with maturity, averaging 13 bp at the 2-year, 31 bp at the 5-year, and 41 bp at the 10-year horizon. This indicates that inflation risk premium in SGBs on average exceeds the liquidity premium in SGBis, inflating BEI. The standard deviation of BEI is 2-3 times larger than the standard deviation of expected inflation which suggests that changes in break-even rates are driven primarily by changes in risk premia. This is confirmed in table 1, where the share of BEI variance explained by the risk premium reaches 61.5% at the 2-year horizon and exceeds 87% at 5-year and 10-year horizons. Inflation expectations and the risk premium are modestly positively correlated at each of the three horizons shown. Figure 1 plots each series at the 2-, 5-, and 10-year maturities. The model suggests that BEI is a reasonable indicator of long term inflation expectations during periods of stable inflation. Between 2012 and 2019, 5- and 10-year risk premium moved between 0 and 50 bp. In periods of market stress however, BEI appears to either over- or understate actual inflation expectations substantially. The sharp drop in Swedish BEI in 2008–2009 is largely attributable to a pronounced fall in the risk premium, which reached approximately -150bp at the 2-year maturity. A natural interpretation is that this reflects a widening liquidity premium on SGBis during the global financial crisis, similar to what studies on US BEI during

this period have found (e.g. Campbell et al. (2009a), D'Amico et al. (2018) and Abrahams et al. (2016)). Notable in the Swedish context however is that this cannot be explained by a large forced seller of inflation-linked securities as with Lehman Brothers in the US. During the inflationary episode of 2022, 2-year expected inflation rose to almost 3% at its peak while long term expectations rose only slightly to around 1.5%. Risk premia rose to 150 bp across all maturities which can plausibly be attributed to higher levels inflation risk.

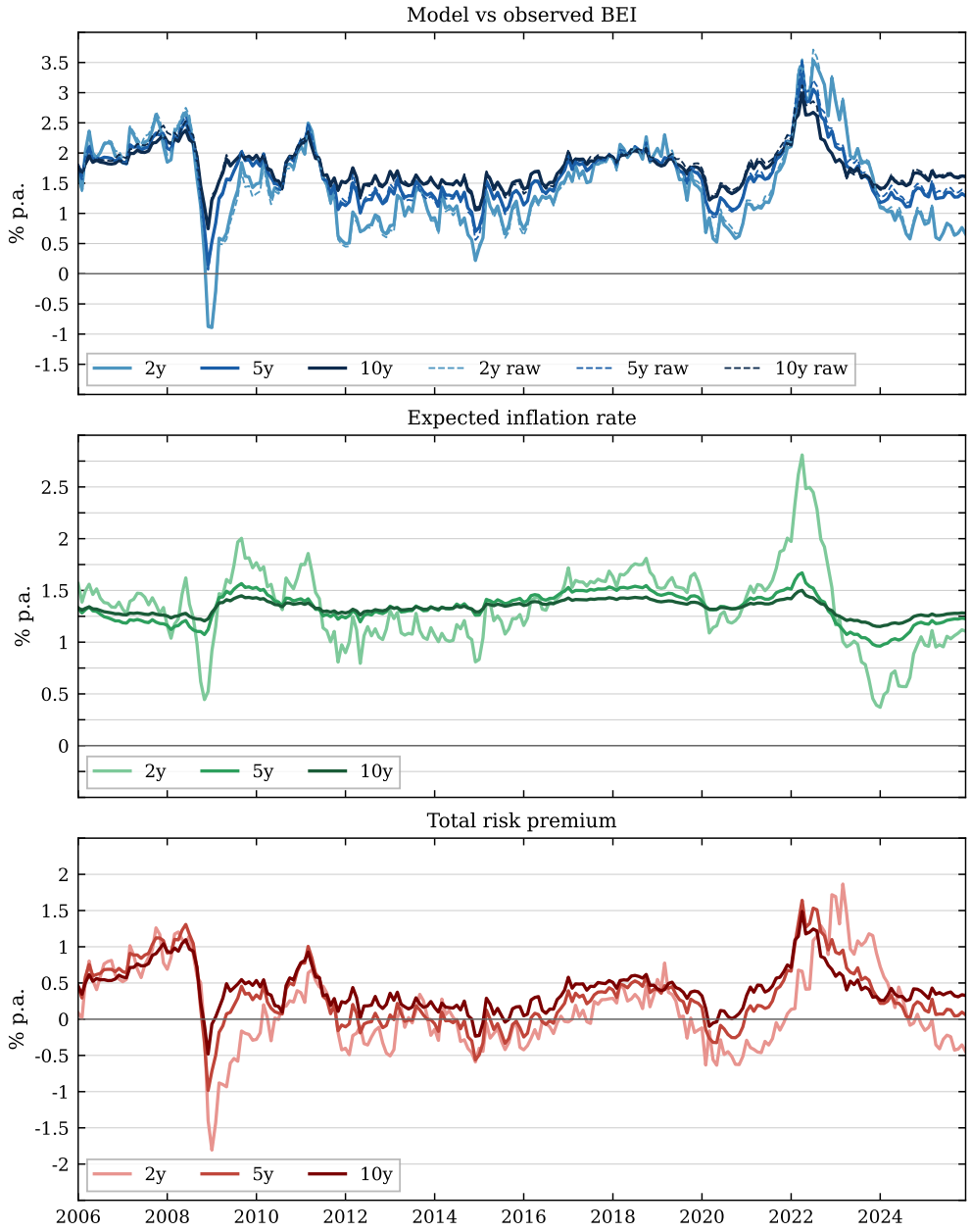


Figure 1: **BEI decomposition, five-factor specification.** The upper panel shows observed BEI (solid) and model-implied BEI (dashed) at 2-, 5-, and 10-year maturities. The middle panel shows model-implied expected inflation and the lower panel shows the model-implied total risk premium. *Source: Authors' calculations based on Bloomberg and Statistics Sweden (SCB) data (2006–2025).*

5.3 Six-factor specification

In the six-factor specification, we include an observable liquidity factor which enables us to identify the time varying liquidity premium in BEI. As highlighted by D'Amico et al. (2018) and Pflueger and Viceira (2013) among others, the liquidity premium is influenced by multiple market conditions. We therefore construct a composite liquidity index $\mathcal{L}_t$ from the equal-weighted average of three different observable measures of current liquidity conditions in the government bond market, in the sprit of Abrahams et al. (2016).

Changes in market risk aversion is a well documented determinant of the liquidity premium. During "flight-to-safety" episodes, investors reduce their risk exposure and demand for low risk assets tends to rise, typically leading to larger yield spreads between risky bonds and government bonds. Although SGBs and SGBis have the same credit risk, the higher level of liquidity risk in inflation-linked bonds is expected to cause a demand imbalance between nominal and inflation-linked bonds when risk aversion rises. A common measure of changes in overall market risk aversion is the near term options implied stock price volatility index VIX[4] which has been found to correlate with the liquidity premium in the US (e.g. Andreasen et al. (2020)) and in Sweden (Alexandersson, 2018). The ratio of relative transaction volumes between SGBs and SGBis is an additional, bond market specific liquidity measure. Lower relative SGBi turnover could imply greater search frictions in the inflation-linked bond market which would motivate a higher liquidity premium. We collect monthly data on average daily secondary-market turnover of SGBs and SGBis from the SNDO, broken down by domestic investors, foreign investors, and primary dealers. Our turnover indicator is the 12-month moving average of the ratio of total SGB to SGBi turnover, aggregated across the three counterparty types. Figure 19 shows that transaction volumes exhibit substantial noise in the short term. Hence, we use the twelve month moving average to better capture long term, structural changes in relative liquidity conditions. Finally, the implied yield spread from bid and ask price quotes – the price premium (discount) compared to the mid-price facing buyers (sellers) of a bond – is commonly seen as an indicator of security-specific trade frictions. We plot the mean bid-ask spreads for one to ten year maturity SGBs and SGBis based on bid-ask price quotes from Bloomberg in figure 18. We question the quality of the data on reported SGBi bid-ask spreads as they are only around 2 bp during the 2000s, when SGBis were new on the market, and rise substantially to 35 bp in 2022. SGB bid-ask spreads on the other hand tend to be below 5 bp and behave more intuitively, rising during the covid-crisis in 2020 and the inflation shock in 2022. We include the SGB bid-ask spreads as our third liquidity measure and interpret it as an indicator of market stress specific to the Swedish bond market. Each of the three liquidity indicators are standardized before computing their equal weighted average. Following Abrahams et al. (2016), we enforce positivity of the composite liquidity index by adding the negative of its series minimum. This is a level normalization that gives high values of $\mathcal{L}_t$ the conventional interpretation of tight liquidity conditions.

The standardized liquidity indicators and the composite liquidity index are plotted in figure 2. The VIX and SGB bid-ask spreads behave similarly, both rising during the covid-crisis, the post-covid inflation shock and what is plausibly the euro-zone debt crisis in the early

[4]Chicago Board Options Exchange, CBOE Volatility Index: VIX [VIXCLS], retrieved from FRED, Federal Reserve Bank of St. Louis; https://fred.stlouisfed.org/series/VIXCLS.

2010s. This supports our interpretation that both series primarily capture changes in market risk sentiment. Notably however, the impact of the global financial crisis is not present in the bid-ask series. The turnover ratio trends downwards during the 2000s and early 2010s, consistent with the growth of the SGBi market. The ratio has been elevated in recent years, possibly related to the SNDO's decision to increase nominal bond issuance and reduce the amount of outstanding inflation-linked debt.

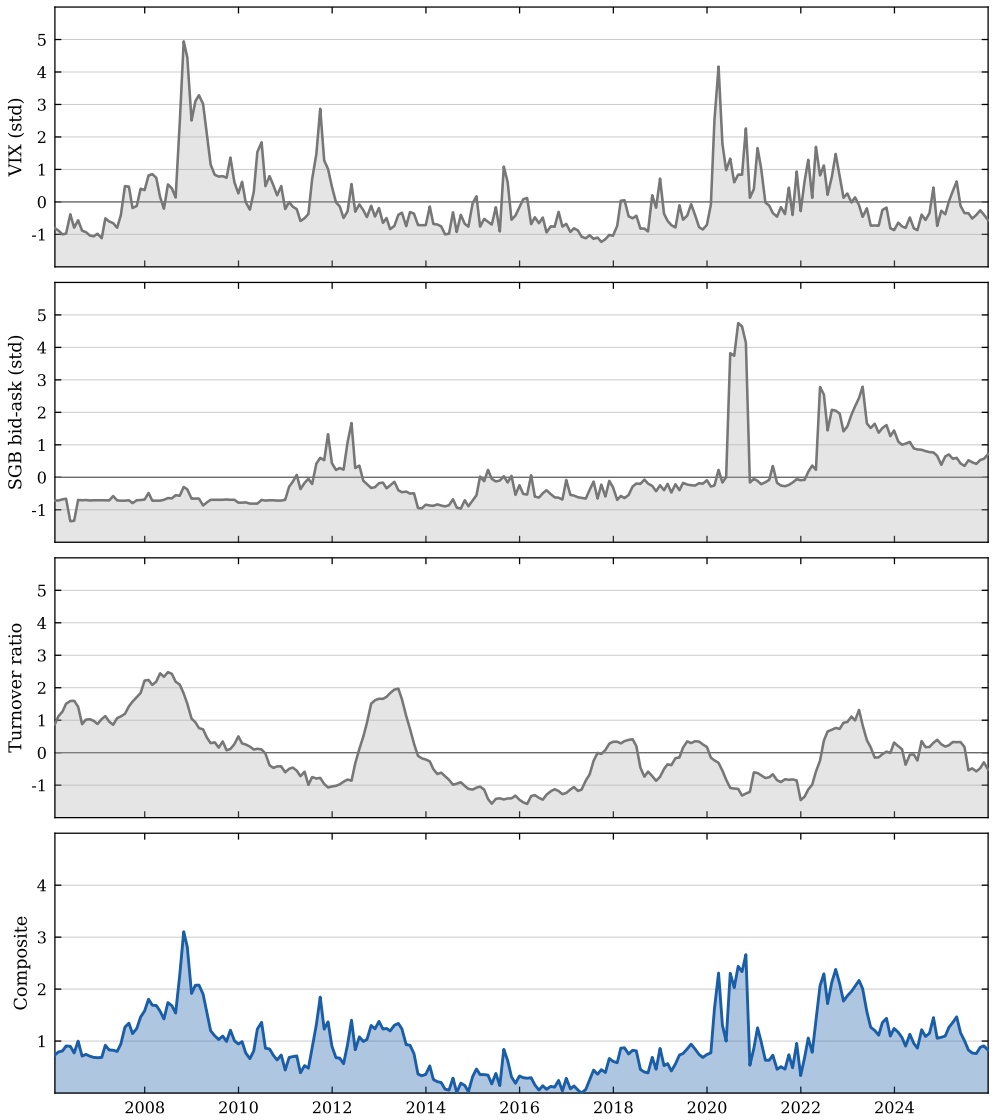


Figure 2: **Composite liquidity index $\mathcal{L}_t$.** The first panel shows the standardized end-of-month VIX index values. The second panel shows the standardized average bid-ask spread for SGBs between 1 year and 10 year maturities. The third panel shows the standardized ratio of 12 month moving average secondary market SGB turnover relative to SGBi turnover from investors and market dealers. The bottom panel plots the equal weighted composite liquidity index. *Source: Authors' rendering of FRED, Bloomberg, and SNDO data (2006–2025).*

The six-factor state vector is $X_t = (X_{N,1,}, X_{N,2}, X_{N,3}, \mathcal{L}, X_{R,1}, X_{R,2})'$: the same three nominal

principal components from the five-factor model, the composite liquidity index, and two orthogonal inflation-linked PCs. The inflation-linked PCs are now extracted from the residuals from a regression on the nominal PCs and the liquidity factor. The inflation-linked PCs are illustrated in figure 17. Yield and excess return fit diagnostics for the six-factor model are presented in table 2. The pooled nominal yield fitting error for the six-factor model is 4.65 bp, comparable to the five-factor model. The pooled inflation-linked yield fitting error falls slightly, 4.67 bp, which suggests that liquidity factor helps explain some inflation-linked yield variation not captured by the five-factor model. It remains highest at the 2-year maturity (7.78 bp). The mean errors are close to zero, indicating no meaningful systematic bias. The yield fitting errors remain highly persistent, with first-order autocorrelations between 0.78 and 0.93. Importantly, return errors are close to zero in mean and show near-zero autocorrelation at both lags across all maturities, consistent with the diagnostic pattern established for the five-factor specification: the factors leave little excess return predictability in the residuals. Estimated and observed nominal and inflation-linked yields are plotted in figure 3.

	Yield fitting error (bp)					Excess return fitting error (bp)				
Maturity	Mean	Std.	RMSE	$\rho(1)$	$\rho(6)$	Mean	Std.	RMSE	$\rho(1)$	$\rho(6)$
Panel A: Nominal bonds										
2Y	0.62	4.83	4.87	0.78	0.27	−0.10	6.77	6.77	−0.20	0.04
5Y	0.79	5.31	5.37	0.93	0.68	0.44	9.80	9.81	−0.09	0.05
10Y	0.38	4.90	4.91	0.78	0.30	−1.61	31.99	32.03	−0.20	0.01
Panel B: Inflation-linked bonds										
2Y	−0.10	7.78	7.78	0.92	0.66	−0.10	6.65	6.65	−0.01	0.00
5Y	0.87	4.06	4.15	0.83	0.47	0.51	11.71	11.72	−0.10	−0.04
10Y	0.78	5.93	5.98	0.89	0.58	−1.16	27.92	27.94	−0.05	−0.05

Table 2: **Fit diagnostics, six-factor specification.** Yield fitting errors (bp) and model-implied excess return fitting errors (bp) at selected maturities. Mean, standard deviation, and RMSE are reported for yield pricing errors (observed minus model-implied zero-coupon yields) and for excess return pricing errors (actual minus model-implied one-month holding period returns from the pricing recursion). $\rho(1)$ and $\rho(6)$ denote first- and sixth-order autocorrelations of the respective error series. *Source: Authors' calculations based on Bloomberg, Statistics Sweden (SCB), FRED, and SNDO data (2006–2025).*

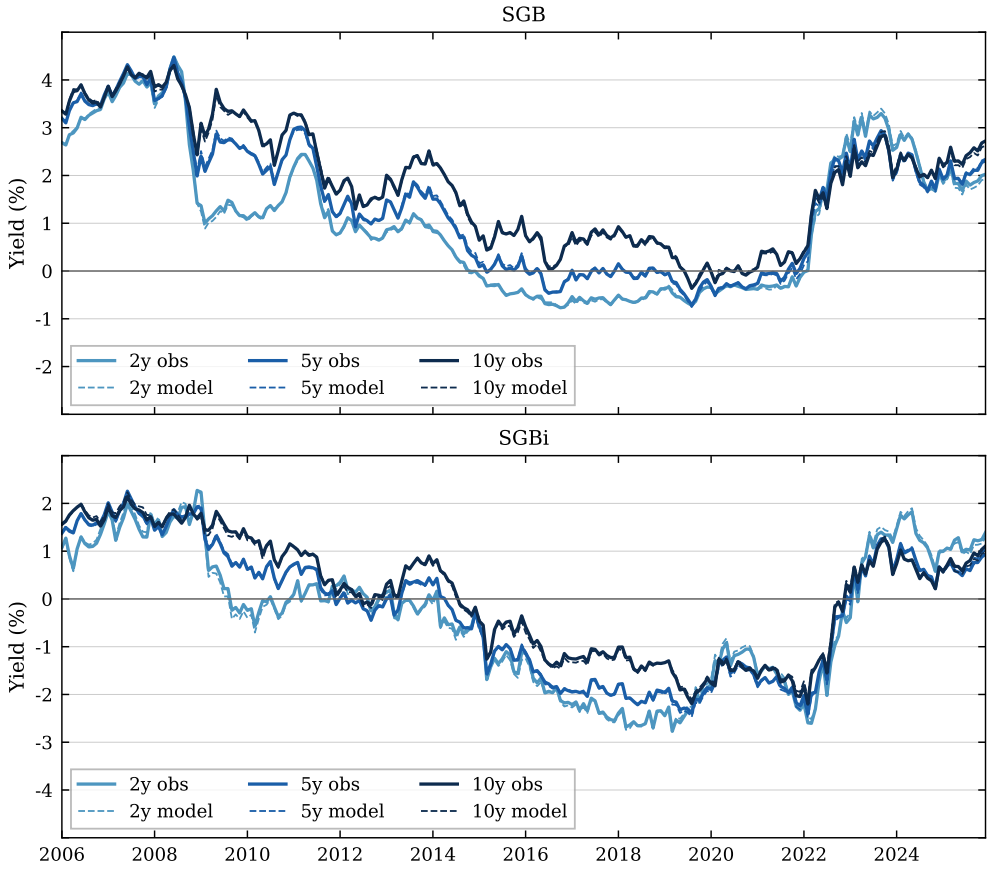


Figure 3: **Observed and estimated zero-coupon yields, six-factor specification.** Solid lines are observed yields and dashed lines are stimated yields at the 2-, 5-, and 10-year maturities. The upper panel shows SGBs and the lower panel shows SGBis. *Source: Authors' calculations based on Bloomberg, Statistics Sweden (SCB), FRED, and SNDO data (2006–2025).*

Table 3 reports Wald statistics for the estimated factor loadings, testing whether the column of $\hat{B}_{\text{gls}}$ associated with each pricing factor is jointly zero across all bond maturities, following Abrahams et al. (2016) and Adrian et al. (2013). For each factor, the test stacks the GLS-estimated return loadings across all maturities into a single vector and asks whether that vector is jointly distinguishable from zero, accounting for the full cross-maturity correlation of pricing errors. Under the null it follows a chi-squared distribution with degrees of freedom equal to the number of maturities tested: $N_{\text{nom}} = 11$ for W_{β_N}, $N_{\text{il}} = 9$ for W_{β_R}, and $N = 20$ for the joint W_β. The three nominal principal components ($\beta_{N,1}$–$\beta_{N,3}$) are strongly significant across both nominal and inflation-linked returns. For the nominal return loadings on the liquidity factor and the two orthogonal principal components, the W_{β_N} statistics are small and none is statistically significant at the 5% level. The inflation-linked W_{β_R} statistics on the other hand are large and strongly significant (11,372.4, 481,135.5, and 247,551.9, all $p = 0.000$). These results align with our expectations. While the nominal PCs explain return variation across both term structures, the orthogonal PCs are constructed to explain unique inflation-linked yield variation. Importantly, this tells us that the liquidity factor contributes significantly to inflation-linked return variation, while it fails to explain a significant share of

nominal returns with $p = 0.277$ and its W_{β_N} being three orders of magnitude smaller than W_{β_R}. This is consistent with the design of $\mathcal{L}$ as an SGBi-specific liquidity indicator. All six factors are individually relevant for the joint cross-section (W_β, all $p = 0.000$), so each contributes explanatory power for returns not already accounted for by the other five factors.

	W_{β_N}	W_{β_R}	W_β
$\beta_{N,1}$	1,041,005.3	488,337.9	1,198,327.6
p-val	(0.000)	(0.000)	(0.000)
$\beta_{N,2}$	485,258.8	136,018.6	522,006.7
p-val	(0.000)	(0.000)	(0.000)
$\beta_{N,3}$	199,939.4	191,728.9	407,719.5
p-val	(0.000)	(0.000)	(0.000)
β_{liq}	13.3	11,372.4	15,146.9
p-val	(0.277)	(0.000)	(0.000)
$\beta_{R,1}$	8.6	481,135.5	686,946.0
p-val	(0.658)	(0.000)	(0.000)
$\beta_{R,2}$	19.1	247,551.9	353,957.6
p-val	(0.059)	(0.000)	(0.000)

Table 3: **Factor significance, six-factor specification.** Wald statistics for the null hypothesis that all return exposures to a given pricing factor are jointly zero. W_{β_N} tests the null across the N_{nom} nominal SGB returns, W_{β_R} across the N_{il} inflation-linked SGBi returns, and W_β across the joint cross-section. p-values in parentheses are based on a χ^2 distribution with degrees of freedom equal to the number of returns in the respective cross-section. $\beta_{N,1}$–$\beta_{N,3}$ are the nominal principal components, β_{liq} is the composite liquidity factor, and $\beta_{R,1}$–$\beta_{R,2}$ are the orthogonalised inflation-linked principal components. *Source: Authors' calculations based on Bloomberg, Statistics Sweden (SCB), FRED, and SNDO data (2006–2025).*

The left panels of figures 4 and 5 plot the estimated factor loadings on yields $-\frac{1}{n}B_n$ for nominal and inflation-linked bonds respectively. The nominal yield loadings confirm the intended factor structure. $X_{N,1}$ loads positively and near-uniformly across all nominal maturities, consistent with its interpretation as a level factor. $X_{N,2}$ loads negatively at short maturities turning positive at longer maturities, characterizing a slope factor. $X_{N,3}$ exhibits the hump-shaped pattern near the 2- and 3-year maturities expected of a curvature factor. Crucially, the liquidity factor X_{liq} and the orthogonalised real components $X_{R,1}$ and $X_{R,2}$ load near zero across the entire nominal maturity spectrum, confirming that these factors have little influence on nominal yield dynamics, consistent with the Wald test evidence in Table 3. The liquidity loadings X_{liq} on inflation-linked yields are highest at short maturities, suggesting that the term structure of the liquidity premium in inflation-linked bonds is downward sloping. $X_{R,1}$ loads positively and near-uniformly across all IL maturities, consistent with a residual level factor for inflation-linked yields, while $X_{R,2}$ loads with opposite sign at the short and long ends, consistent with a residual slope factor.

The right panels of the figures plot the one-month excess return loadings $B_n'\lambda_1$ on each factor, where $\lambda_1 = \Phi - \tilde{\Phi}$ collects the estimated time varying prices of factor risk. A positive entry

indicates that a positive shock to the factor raises the expected one-month excess return on an m-maturity bond. Three things stand out. First, the curvature factor $X_{N,3}$ has the largest absolute excess return loadings for both long-maturity nominal and inflation-linked bonds, despite its limited contemporaneous impact on yields. Higher curvature predicts lower expected excess returns at long maturities. Second, based on the increasing excess return loadings on the second principal component, a positively sloping yield curve predicts positive excess returns on long maturity nominal and inflation-linked bonds, consistent with the findings in Campbell and Shiller (1991) and Fama and Bliss (1987). Note also that this holds for both slope factors $(X_{N,2}, X_{R,2})$ on both nominal and inflation-linked bonds. Third, the liquidity factor carries small excess return loadings, meaning that a drop liquidity does not predict higher one-month excess returns. The estimated loadings suggest that exposure to time-varying liquidity risk in SGBis is not rewarded by higher returns in the near term.

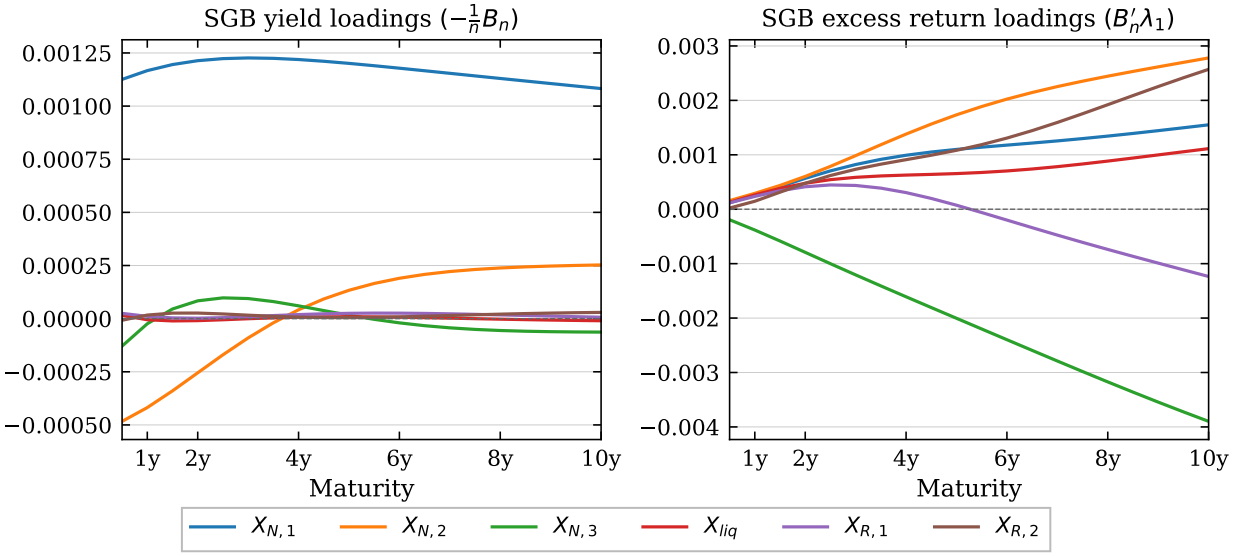


Figure 4: **Factor loadings, nominal bonds.** Left panel plots the implied yield loadings $-\frac{1}{n}B_n$, interpreted as the response of the n-year nominal yield to a contemporaneous unit shock to each pricing factor. Right panel plots the excess return loadings $B_n'\lambda_1$, interpreted as the response of the expected one-month excess holding return on an n-year nominal bond to a unit factor shock. *Source: Authors' calculations based on Bloomberg, Statistics Sweden (SCB), FRED, and SNDO data (2006–2025).*

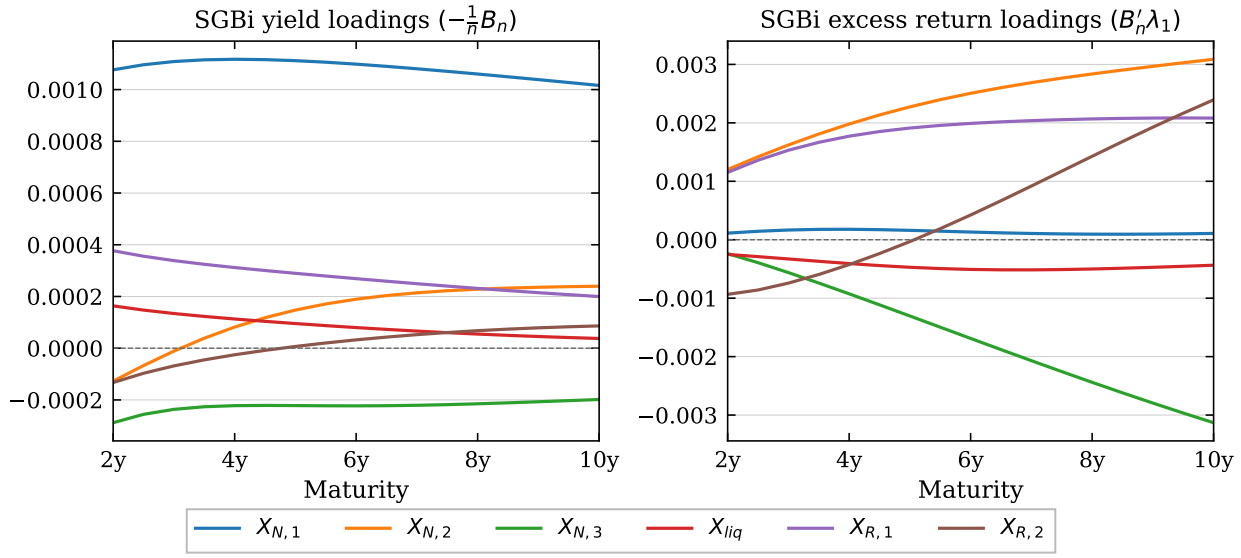


Figure 5: **Factor loadings, inflation-linked bonds.** Left panel plots the implied yield loadings $-\frac{1}{n}B_{n,R}$, interpreted as the response of the n-year real yield to a contemporaneous unit shock to each pricing factor. Right panel plots the excess return loadings $B_{n,R}'\lambda_1$, interpreted as the response of the expected one-month excess holding return on an n-year inflation-linked bond to a unit factor shock. *Source: Authors' calculations based on Bloomberg, Statistics Sweden (SCB), FRED, and SNDO data (2006–2025).*

Table 4 reports summary statistics for the three-way BEI decomposition. Average expected inflation increases by 5 bp to 1.38% across all maturities when adjusting for liquidity. The estimated inflation expectations remain well below the 2%-target. This can partly be explained by the persistently low CPI inflation during the 2010s which cover the majority of our sample period. In section 5.3.1 we compare our estimated inflation expectations to other inflation forecasters. The liquidity premium component in BEI is negative and it decreases with maturity, averaging -22bp at the 2-year, -11bp at the 5-year, and -5bp at the 10-year maturity. The inflation risk premium is on average positive and increases with maturity, from 19 bp at the 2-year to 44 bp at the 10-year horizon. BEI variation is primarily driven by time varying inflation risk premia, especially at longer maturities. The standard deviation of 10-year inflation risk premia is 30 bp while 10-year inflation expectations have a standard deviation of only 7 bp. In addition, the positive but weak correlation between inflation risk premia and inflation expectations in table 5 means that a rising inflation risk premium is not strongly associated with rising inflation expectations.

The full decomposition is plotted in figure 6. The decomposition shows that risk premia behaved differently during two periods of market stress in our sample: the global financial crisis 2008-2009 and the post-covid inflation shock of 2022-2023. According to our estimates, the 2-year inflation risk premium bottomed out at -150 bp and the 2-year liquidity premium at roughly -75 bp during the global financial crisis, explaining most of the drop in short-term BEI. Long-term BEI also fell substantially, driven almost entirely by lower inflation risk premia as long-term inflation expectations remained stable. The sharp fall in inflation risk premia, briefly turning negative, is consistent with nominal bonds providing a hedge against deflationary recession risks, seen as bond yields fell during this episode (see figure 3). This

view is also consistent with greater SGBi liquidity premia in response to higher risk aversion. The 2022-2023 inflation shock generated the opposite pattern. Inflation risk premia rose to 150-200 bp while the short term liquidity premium fell to -50 bp. Nominal bond yields rose sharply during this period, providing a poor hedge against the stagflationary risks. Hence, the sign reversal in inflation risk premia across the two episodes can plausibly be explained by a positive covariance between inflation shocks and consumption growth (Piazzesi and Schneider, 2006) and equity returns (Campbell et al., 2009b) in 2008-2009, and a negative covariance in 2022-2023. Nominal bonds hedged consumption and equity risk during the financial crisis and failed to do so during the recent inflation shock.

	EI		*LP*		*IRP*		*BEI*	
Maturity	Mean	Std.	Mean	Std.	Mean	Std.	Mean	Std.
Panel A: 5-factor model								
2Y	1.34	0.39	—	—	0.13	0.56	1.47	0.72
5Y	1.33	0.15	—	—	0.31	0.43	1.64	0.46
10Y	1.33	0.07	—	—	0.41	0.29	1.75	0.31
Panel B: 6-factor model								
2Y	1.38	0.38	−0.22	0.14	0.19	0.59	1.46	0.72
5Y	1.38	0.15	−0.11	0.07	0.37	0.45	1.67	0.46
10Y	1.38	0.07	−0.05	0.03	0.44	0.30	1.78	0.31

Table 4: **BEI decomposition summary statistics, both specifications.** Mean and standard deviation are reported in percent per annum for model-implied expected inflation (EI), liquidity premium (LP), inflation risk premium (IRP), and model-implied BEI at 2-, 5-, and 10-year horizons. *Source: Authors' calculations based on Bloomberg, Statistics Sweden (SCB), FRED, and SNDO data (2006–2025).*

	Cross-correlations			Correlations with BEI		
Maturity	$\rho(EI, LP)$	$\rho(EI, IRP)$	$\rho(LP, IRP)$	$\rho(EI)$	$\rho(LP)$	$\rho(IRP)$
2Y	0.218	0.082	−0.379	0.612	−0.101	0.833
5Y	0.404	−0.011	−0.345	0.352	−0.092	0.927
10Y	0.412	0.120	−0.278	0.382	−0.084	0.960

Table 5: **BEI correlations, six-factor specification.** *Left:* Pairwise correlations between EI, LP, and IRP. *Right:* Correlation of each component with BEI, at the 2-, 5-, and 10-year maturities. *Source: Authors' calculations based on Bloomberg, Statistics Sweden (SCB), FRED, and SNDO data (2006–2025).*

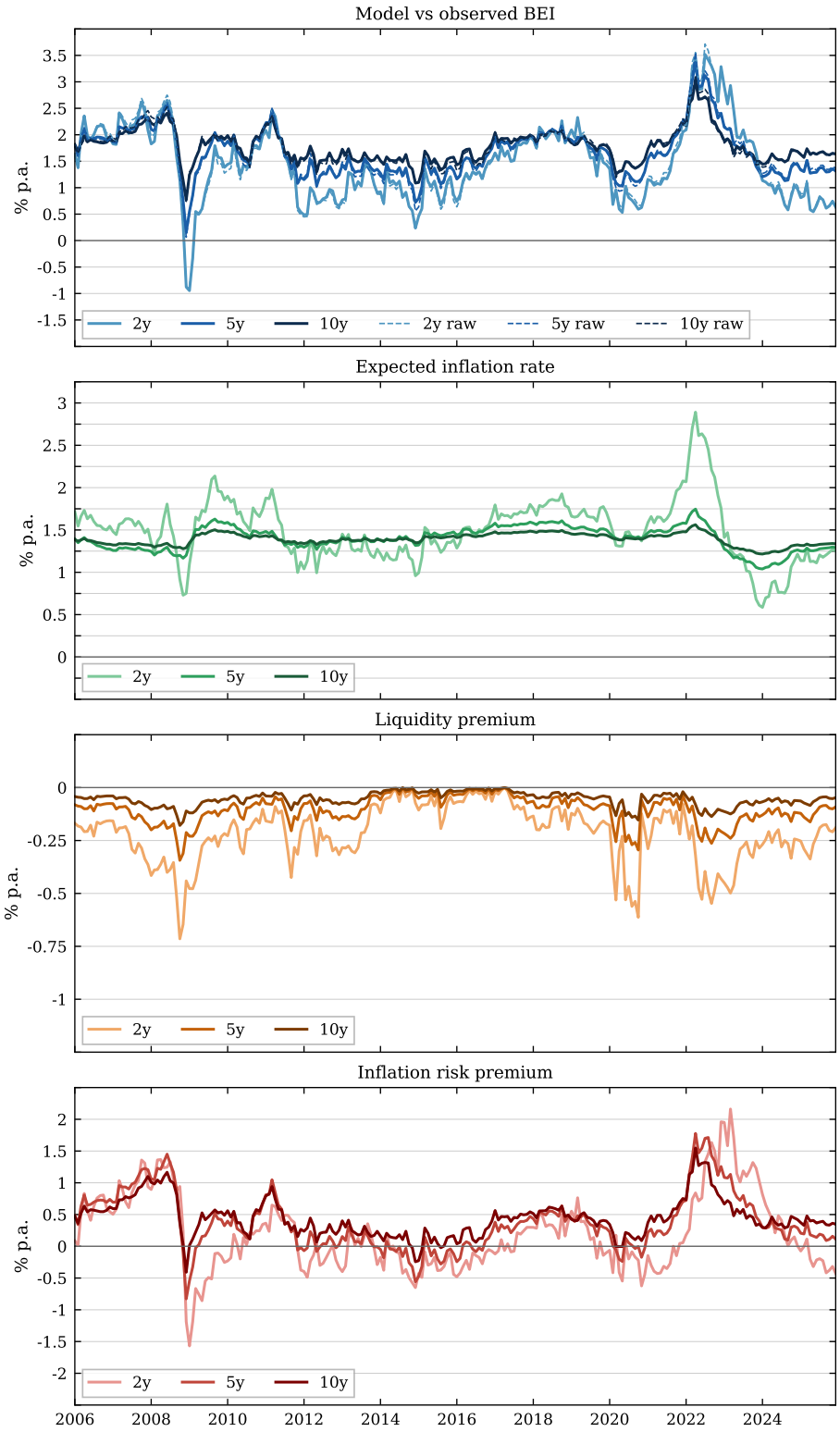


Figure 6: **BEI decomposition, six-factor specification.** The upper panel shows observed BEI (solid) and model-implied BEI (dashed) at 2-, 5-, and 10-year maturities. The second panel shows model-implied expected inflation under the $\mathbb{P}$-measure. The third panel shows the liquidity premium. The lower panel shows the liquidity-adjusted inflation risk premium. *Source: Authors' calculations based on Bloomberg, Statistics Sweden (SCB), FRED, and SNDO data (2006–2025).*

5.3.1 Inflation forecasting with the six-factor specification

One motivation for the decomposition of BEI into expected inflation and risk premium components in the previous section was to obtain a distortion free market based measure of inflation expectations. An informative way to evaluate our model is therefore to compare the inflation forecasting ability of estimated inflation expectations against BEI. Table 6 shows the CPI forecasting performance of four different series: estimated inflation expectations from the six-factor model, observed BEI, survey expectations, and a benchmark random walk model. Forecasting performance is evaluated by root mean squared CPI prediction errors in basis points. The models are evaluated monthly by comparing the 2 and 5-year inflation forecasts, and the 5-year spot inflation forecast (annual inflation five years ahead), against realized CPI inflation over the corresponding periods. Commissioned by the Riksbank, Origo Group (Kantar Prospera from 2006 to 2025) publishes monthly surveys on the 1, 2 and 5 year inflation expectations of money market players. Until 2010, surveys were conducted quarterly. Because we do not estimate BEI at shorter maturities than 2 years, we only include the 5 year survey forecasts in the comparison. The random walk model uses the rolling backward looking m-period inflation to forecast inflation over the next m-periods. For the spot forecast, the random walk model uses rolling twelve month realized inflation. First we conduct the forecasting exercise using the full sample to estimate our model. We then perform the same exercise but out-of-sample, re-estimating the entire model each month based only on the data available up until that point, with a four year training period 2006-2010, and evaluating the model's 2 and 5-year forecasts and the 5-year spot forecast at each step. The in-sample and out-of-sample exercises are also performed over a shorter sample ending December 2022 to avoid the effect of the unanticipated post-covid inflation shock.

In-sample, the estimated inflation expectations produce the lowest RMSE at 2 and 5-year horizons in both the full period and the pre-2022 sample. BEI produces the best 5-year spot forecast over the full sample, but the six-factor model produces the best spot forecast in the shorter sample. No model anticipates the post-covid inflation shock, with forecast errors often being 100 bp larger in the full sample exercise compared to the truncated sample forecasts. Out-of-sample however, our model performs worse than both BEI and survey forecasts in both samples. Surprisingly, BEI slightly outperforms survey forecasts in the out-of-sample exercise, where the samples are four years shorter compared to the in-sample exercise. The random walk model consistently performs worst, indicating that all three forward-looking measures contain meaningful information about future inflation. Based on the results, we conclude that the risk adjusted break even rates improve the in-sample inflation expectations fit without translating into superior out-of-sample forecasts. The poor out-of-sample performance may in part reflect parameter instability under monthly re-estimation with limited training data, especially early in the out-of-sample period.

	Evaluated to 2025-12			*Evaluated to 2021-12*		
Series	2y avg	5y avg	5y spot	2y avg	5y avg	5y spot
In-sample						
BEI	222.9	141.8	270.7	101.7	81.4	138.8
EI 6-factor	210.3	138.9	280.9	84.5	57.9	107.6
Survey	—	—	289.3	—	—	127.7
Random walk	286.0	169.6	293.7	142.8	85.0	182.9
N	216	180	180	168	132	132
Out-of-sample						
BEI	250.2	162.6	304.2	84.3	76.9	80.0
EI 6-factor	255.7	190.9	350.2	98.4	88.0	104.6
Survey	—	—	306.5	—	—	84.8
Random walk	319.5	203.0	329.0	124.9	100.1	161.3
N	156	120	120	108	72	72

Table 6: **Root mean squared prediction errors in basis points for average future CPI inflation at the 2- and 5-year horizons, and 5 year spot inflation.** *BEI* is the observed breakeven inflation rate. *EI 6-factor* is the model-implied expected inflation. *Survey* are the official survey inflation expectations published by Origo Group and Kantar Prospera. *Random walk* is a benchmark model predicting future inflation based on current inflation. *Source: Authors' calculations based on Bloomberg, Statistics Sweden (SCB), FRED, SNDO, and Origo Group/Kantar Prospera data (2006–2025).*

5.3.2 Impact from the indexation lag

Figure 7 plots the annualized contribution of the carry component in SGBi yields, $\frac{12}{m}Q_t/Q_{t-3}$, to BEI. The annualized carry lowers SGBi yields and inflates BEI by equal amounts. As established in section 3.4, because the model treats inflation-linked bonds as perfectly indexed and does not separately identify the carry contribution, the carry is absorbed into the estimated BEI components. This is expected to bias the estimates if the realized inflation rate over the past three months does not match the expected inflation rate for the final three months before the bond matures. For reference, an annualized inflation rate over the past three months of 2% implies carry contribution to 2-year, 5-year and 10-year BEI of +25 bp, +10 bp and +5 bp respectively. Assuming that long-term inflation rates are well anchored around 2%, then annualized carry contributions close to this range should not have any meaningful impact on the model estimates. During the period of stable inflation in the 2010s, the carry tended to be small at all maturities, and the model's treatment of SGBi yields as frictionless real yields is approximately valid. In 2022-2023, the 2-year carry contribution goes to almost +175 bp as CPI inflation spiked, comparable to the estimated rise in 2-year inflation risk premia and inflation expectations during the same period, documented in in 5.3. Hence, short term inflation risk premia and expected inflation are likely overstated. The inflation risk premium is the most responsive of the estimated components and is possibly therefore most impacted by the carry distortion. Since the liquidity premium is identified from the liquidity factor, which does not depend on SGBi yields directly, the estimated liquidity premium should not be as sensitive to the carry distortions. The 5 and 10-year carry contributions peak at approximately 70 and 35 bp respectively, representing a proportionally smaller distortion

relative to the estimated long-horizon inflation risk premia and inflation expectations, making them more reliable.

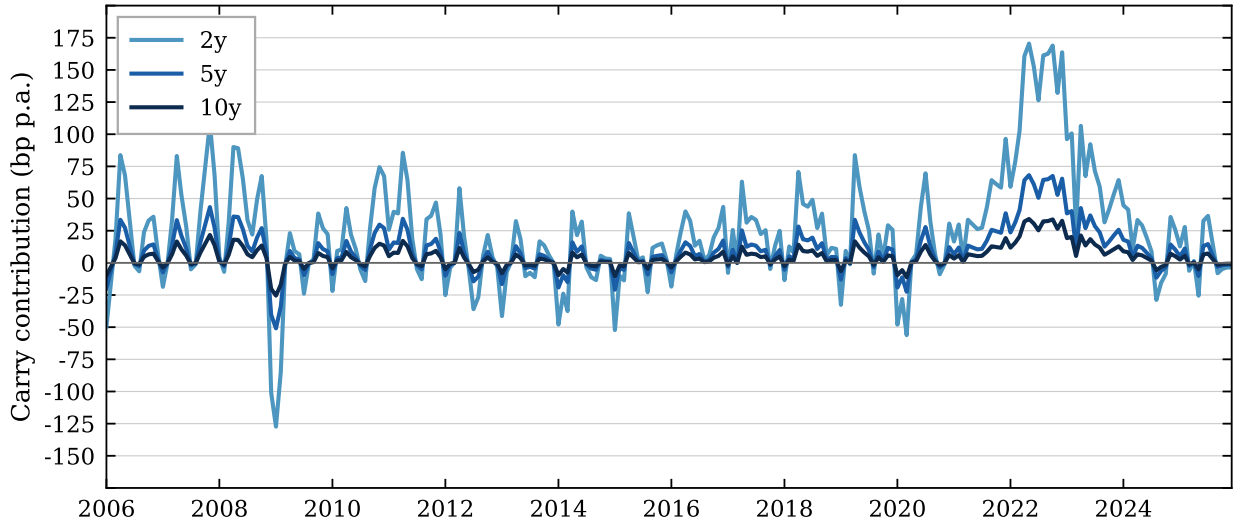


Figure 7: **Annualized contribution of the carry component** (three-month accrued CPI inflation compensation) in SGBi yields to BEI at 2-year, 5-year and 10-year maturities. *Source: Authors' calculations based on Bloomberg, Statistics Sweden (SCB), FRED, and SNDO data (2006–2025).*

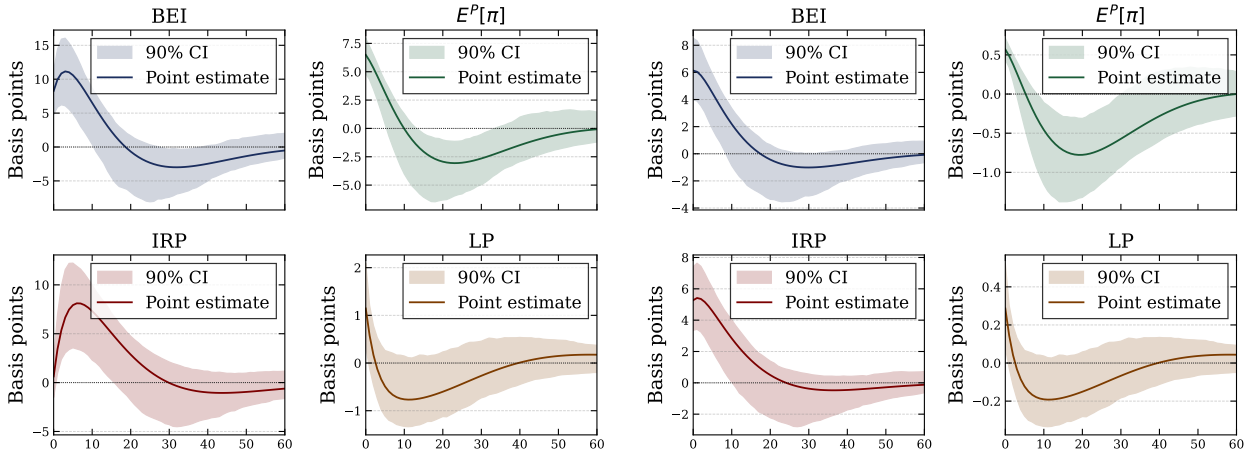
5.4 IRF analysis of the six-factor specification

We conduct an IRF analysis to trace the dynamic response of BEI and its three components to shocks in the pricing factors. The exercise serves two purposes. First, it provides an economic validation of the model: if the decomposition is economically meaningful, the dynamic response in BEI to a liquidity shock should primarily be though liquidity premia, and a yield level shock is expected to influence short term inflation expectations and inflation risk premia. Second, bootstrap confidence bands allow us to assess which features of the impulse responses are robust across repeated re-estimation, and which are sensitive to the specific sample used.

The pricing factors X_t are assumed to follow a Gaussian VAR(1) (see equation (1)). Because the factor shocks v_t are contemporaneously correlated, we orthogonalize them by a Cholesky decomposition: $\Sigma = PP', \varepsilon_t = P^{-1}v_t \sim \mathcal{N}(0, I_K)$, where P is lower-triangular. The following order is imposed: $\left(X_{N,1},\ X_{N,2},\ X_{N,3},\ \mathcal{L},\ X_{R,1},\ X_{R,2}\right)$, where shocks to factors ordered earlier are allowed to have contemporaneous effect on the other factors. The nominal principal components are placed first with an ordering that corresponds to their explanatory power of nominal yields. We place the liquidity factor before the inflation-linked principal components, which are placed last. In section 5.3 we find evidence that changes in liquidity conditions do influence inflation-linked yields, but have a limited impact on nominal yields. The IRF for the shock over h-periods is given by: $\Phi^h P e_k$, where e_k is the k-th standard basis vector. The impulse responses are transmitted into estimated BEI, inflation expectations, inflation risk premia and liquidity premia through their loadings on the pricing factors.

The factor coefficients in the expressions for BEI, expected inflation, inflation risk premia and liquidity premia are respectively: $i)$ $-\frac{1}{m}(B_m - B_{m,R})$, $ii)$ $-\frac{1}{m}(B_m^{\mathbb{P},(-\mathcal{L})} - B_{m,R}^{\mathbb{P},(-\mathcal{L})})'$, $iii)$ $-\frac{1}{m}\Big((B_m^{(-\mathcal{L})} - B_{m,R}^{(-\mathcal{L})})' - (B_m^{\mathbb{P},(-\mathcal{L})} - B_{m,R}^{\mathbb{P},(-\mathcal{L})})'\Big)$ and $iv)$ $-\frac{1}{m}(b_m^{\mathcal{L}} - b_{m,R}^{\mathcal{L}})$ (see section 3.3). The dynamic response to estimated BEI and its components from a standard deviation shock in a factor is derived by projecting the IRF onto these coefficients. We report the dynamic responses in annualized rates by scaling the coefficients by a factor of 12. Responses are reported at the 2-year and 10-year maturities over a 60-month horizon. Confidence bands are constructed via a moving-block bootstrap on the VAR residuals (Künsch, 1989; Brüggemann et al., 2016). Because Φ^h makes IRFs nonlinear in the estimated VAR parameters, standard asymptotic inference is unreliable. For each of $B = 500$ draws, residuals $\{\hat{v}_t\}$ are resampled in blocks of 12 consecutive months to preserve within-year dependence. A pseudo-sample is then reconstructed recursively, and $\Phi^{(b)}$ and $\Sigma^{(b)}$ are re-estimated by OLS, holding the ATSM pricing coefficients fixed at their full-sample values. IRFs are computed for each draw, and the 5th and 95th percentiles form 90% bands. Because the pricing recursion is held fixed, the bands capture sampling uncertainty in how shocks propagate through Φ but treat the estimated risk-neutral parameters as known, and therefore constitute a lower bound on total estimation uncertainty.

5.4.1 Level shock



(a) 2-year maturity

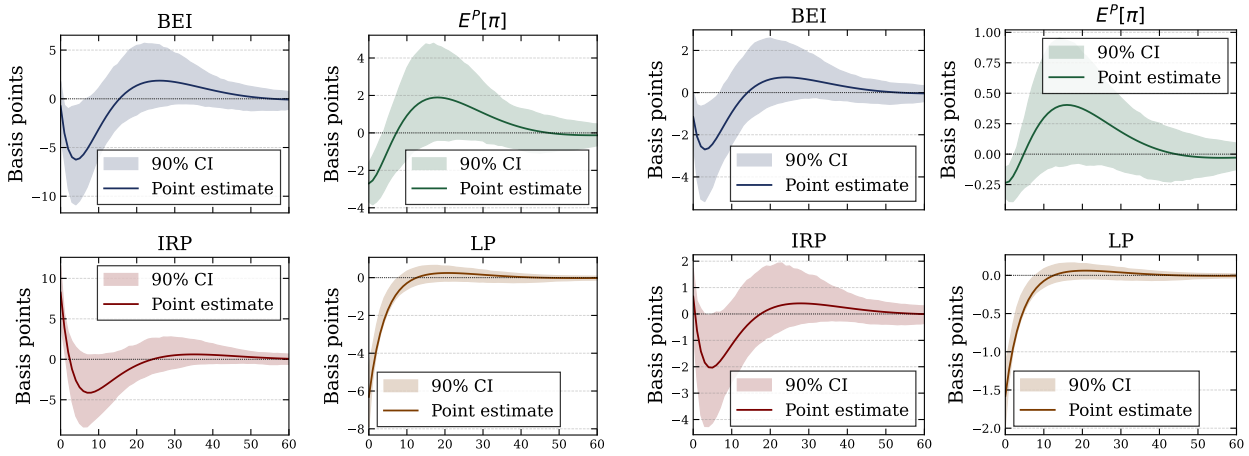
(b) 10-year maturity

Figure 8: **IRF to a one-standard-deviation shock to the nominal level factor (PC1).** Shaded bands are 90% moving-block bootstrap confidence intervals. Horizon in months on the horizontal axis. *Source: Authors' calculations based on Bloomberg, Statistics Sweden (SCB), FRED, and SNDO data (2006–2025).*

Shocks to the level factor shift the entire yield curve and can economically be interpreted as changes to the short rate in the economy. A positive level shock has a contemporaneous effect on 2-year BEI of roughly +11 bp, driven by a rise in inflation risk premia (IRP) and inflation expectations ($E^{\mathbb{P}}[\pi]$). This could be interpreted in a context where short rates rise in response to high inflation. The IRP contribution peaks at around +8 bp after 5–10 months, and its confidence band lies above zero for roughly the first 15 months. $E^{\mathbb{P}}[\pi]$ contributes

around +7 bp on impact but its confidence band crosses zero within the first eight to ten months and the point estimate turns negative thereafter. The responses suggest that a rise in the short rate causes short term inflation expectations to fall initially and mean revert in the long term, consistent with how monetary policy tends to be executed when inflation is above target. The liquidity premium response is indistinguishable from zero throughout. The response to 10-year inflation expectations follow a similar pattern, but it is 5 to 10 times smaller, consistent will well anchored long term inflation expectations. There is however an economically and statistically significant contemporaneous rise in long term BEI that is almost entirely driven by a rise in IRP. This supports our finding in 5.3 that variation in long term BEI is primarily caused by time varying inflation risk premia.

5.4.2 Liquidity shock



(a) 2-year maturity

(b) 10-year maturity

Figure 9: **IRF to a one-standard-deviation shock to the composite liquidity factor.** Shaded bands are 90% moving-block bootstrap confidence intervals. Horizon in months on the horizontal axis. *Source: Authors' calculations based on Bloomberg, Statistics Sweden (SCB), FRED, and SNDO data (2006–2025).*

A liquidity shock compresses 2-year BEI by roughly −6 bp on impact, though the confidence band is barely, and only for a short time, below zero. The liquidity premium in BEI falls sharply by roughly the same amount. The liquidity response is statistically significant for up to 10 months, after which there is no impact. The responses indicate that the model successfully identifies time varying liquidity premia and that the constructed liquidity factor works as intended. A positive shock to the liquidity factor raises inflation-linked yields relative to nominal yields, compressing BEI, without impacting inflation expectations or inflation risk premia in any meaningful way. The responses to inflation expectations and IRP are barely significant on impact. The results also tell us that responses of the liquidity premium to changes in liquidity conditions tend to be short lived. This aligns with the behavior of the composite liquidity index in figure 2 where changes in market risk aversion, measured by the VIX and nominal bid-ask spreads, are for the most part temporary in nature. For 10-year maturities, the results are qualitatively similar but the magnitude is considerably smaller. This matches our earlier finding that long maturity inflation-linked bonds and BEI are less

sensitive to changes in liquidity conditions and that the liquidity premium term structure is in average downward sloping.

5.4.3 Robustness to Cholesky ordering

Our baseline ordering places the liquidity factor after the nominal principal components but before the inflation-linked PCs. To assess how sensitive our results are to the specific ordering, we re-run all IRFs under two alternative orderings: placing $\mathcal{L}_t$ first, before all nominal PCs, and placing $\mathcal{L}_t$ last, after the inflation-linked PCs. For the level shock, the BEI and IRP responses are virtually identical across all three orderings, and the expected inflation response maintains its direction and remains short-lived in each case. For the liquidity shock, the immediate impact on the liquidity premium becomes greater in magnitudes at both the 2- and 10-year maturities but the shape of the response is preserved regardless of where $\mathcal{L}_t$ enters the ordering. Taken together, the economic conclusions are robust to the identification scheme. Level shocks impact IRP and inflation expectations in the short term, and mainly impact IRP in the long term. Liquidity shocks compress BEI through the liquidity premium channel.

6 Discussion and conclusions

We estimate the joint nominal and inflation-linked affine term structure model of Abrahams et al. (2016) on Swedish data over 2006-2025. The model is implemented in two specifications. The benchmark five factor specification uses three principal components from nominal SGB yields and two orthogonalized principal components from inflation-linked SGBi yields, and decomposes BEI into expected inflation and a risk premium component. In our preferred model, the six factor specification, we include a composite liquidity index which enables a separate identification of the liquidity premium. Model implied expected-inflation is essentially identical across both specifications, with the liquidity adjusted expected inflation of the six factor model averaging 1.38% at 2-year, 5-year and 10-year horizons. This is notably lower compared to the results of similar studies on euro-area and US inflation expectations such as Hördahl and Tristani (2012) and Christensen et al. (2010) who report 10-year inflation expectations around 2%. This is in part attributable to the specific time period studied, where our sample, in contrast to most earlier studies, covers the 2010s when inflation was persistently low. Our estimates of the average liquidity adjusted inflation risk premium are 19 bp, 37 bp and 44 bp at the 2-, 5- and 10-year horizons. These estimates are comparable to e.g. Hördahl and Tristani (2012) who estimate the average 10-year inflation risk premium in the euro area to 20 bp, and who also find that the inflation risk premium tends to increase with maturity. The estimated time varying liquidity premium component in BEI averages -22 bp, -11 bp and -5 bp at the 2-, 5- and 10-year maturities, which is lower in magnitude compared to US studies like D'Amico et al. (2018) and Abrahams et al. (2016) who find that the TIPS liquidity premium rose to 200 bp during the financial crisis in 2008. Similar to these studies however, our estimated liquidity premium is particularly sensitive to changes in market risk aversion, due to the inclusion of the VIX and SGB bid-ask spreads in the liquidity factor. Furthermore, our finding that the liquidity premium term structure is downward sloping implies that short maturity SGBi yields are most sensitive to shifts in market risk aversion. One reason for this could be the transitory nature of the liquidity shocks captured by our liquidity index. It could

however also be indicative of higher demand from institutional buy-and-hold investors for long maturity inflation-linked bonds, consistent with the mechanism highlighted in Andreasen et al. (2020).

Our results suggest that variation in Swedish BEI is primarily driven by risk premia, and that time varying inflation risk premia explains almost all variation in long term BEI. These tendencies are particularly striking during the two episodes of severe market stress in our sample. During the 2008–2009 global financial crisis, the 2-year inflation risk premium bottomed out at around -150 bp and the 2-year liquidity premium at -75 bp. The 10-year inflation risk premium also fell substantially, briefly turning negative, while long horizon expected inflation remained anchored. During the inflation shock of 2022-2023, both short- and long-term inflation risk premia rose to 150–200 bp and the short-term liquidity premium fell to -50 bp. The reversal in the inflation risk premium across the two episodes is suggestive of changes in the hedging properties of nominal bonds with regards to consumption risk and equity risk, consistent with the mechanisms in Piazzesi and Schneider (2006) and Campbell et al. (2009b) respectively. During the financial crisis, SGBs provided an attractive hedge against deflationary recession risks, motivating lower inflation risk premia. During the inflation shock in 2022-2023 however, SGBs did not hedge the stagflationary risks as their real returns fell, leading to a sharp rise in inflation risk premia. Across both episodes, model-implied long horizon expected inflation remained close to its sample mean, indicating that long term inflation expectations in Sweden remained well anchored throughout. The point estimates of our estimated inflation risk premium and inflation expectations should however be interpreted with some caution, especially during 2022-2023. As documented in section 5.3.2, the annualized carry contribution to BEI stemming from the indexation lag, which the model does not account for, rose to almost 175 bp during the inflation spike, most of which we argue was absorbed into the estimated short-end inflation risk premium and expected inflation. As a result, our short-term BEI decomposition over this period is subject to substantial carry distortion, leading to overstated components. The impulse response analysis conducted in section 5.4 however offers economic validation to the BEI decomposition. A shock to the level factor, interpreted as a rise in short-term interest rates, causes short term inflation expectations and inflation risk premia to fall in the short term, with no significant impact past 10-20 months. The level shock mainly affects long term BEI through inflation risk premia and generates only a small response in long term inflation expectations, reinforcing our earlier result that long-term inflation expectations have been anchored. The dynamic response of BEI to a liquidity shock is short lived, barely statistically significant, and is almost entirely driven by a transitory rise in the liquidity premium.

In light of the announcement from the SNDO to reduce the amount of outstanding inflation-linked debt to 80 billion SEK by the end of 2029, a smaller SGBi market is likely to amplify the liquidity distortions in BEI documented here. SGBi transaction volume relative to SGB transaction volume in the secondary market was low at the beginning of our sample which contributed to above average levels of liquidity premia. Furthermore, a reduction in the amount of traded inflation-linked debt will probably cause liquidity premia to become even more sensitive to changes in market risk sentiment. The informational content of BEI as a real-time indicator of long term inflation expectations, while already limited and unreliable

during market stress, is therefore likely to deteriorate further. This strengthens the case for routinely complementing BEI with a model-based decomposition and with survey expectations when assessing inflation expectations in Sweden. It is worth noting however that, according to our estimates, at longer maturities the average inflation risk premia in nominal bonds far exceeds the average liquidity premium present in inflation-linked bonds. This suggests that, contrary to the cost rationale stated by the SNDO, inflation-linked bonds may in fact constitute a relatively cheap funding alternative.

Several limitations of our analysis suggest avenues for further research. The model fails to account for the indexation lag inherent in inflation-linked bonds, in particular following the 2022-2023 inflation shock, which makes our decomposition of short term BEI less reliable. We encourage future studies similar to ours to explore specifications that identify and separate the indexation lag carry contribution to BEI. Future research should also explore how SGBi liquidity premia respond to different liquidity measures. Most of the variation in liquidity conditions in our model is generated by the VIX index and the SGB bid-ask spread, both of which are interpreted as measures of market stress. That our estimated time varying liquidity premium is smaller compared to the far deeper and more developed inflation-linked bond market in the US might be a sign that our liquidity factor does not include important determinants of liquidity conditions in the Swedish SGBi market. Other measures, such as use of the SNDOs repo facility for SGBis as an alternative measure of search frictions in the secondary market, as proposed by Alexandersson (2018), or measures that capture the funding costs for arbitrageurs, highlighted in Pflueger and Viceira (2013), will likely capture additional liquidity related variation in SGBi yields.

References

Abrahams, M., Adrian, T., Crump, R. K., Moench, E., and Yu, R. (2016). Decomposing real and nominal yield curves. *Journal of Monetary Economics*, 84:182–200.

Adrian, T., Crump, R. K., and Moench, E. (2013). Pricing the term structure with linear regressions. *Journal of Financial Economics*, 110(1):110–138.

Alexandersson, L. (2018). Liquidity premiums in the Swedish inflation-indexed government bond market. *Sveriges Riksbank Economic Review*, (2):82–93.

Andreasen, M. M., Christensen, J. H. E., and Riddell, S. (2020). The TIPS liquidity premium. Working Paper 2017-11, Federal Reserve Bank of San Francisco.

Ang, A. and Piazzesi, M. (2003). A no-arbitrage vector autoregression of term structure dynamics with macroeconomic and latent variables. *Journal of Monetary Economics*, 50(4):745–787.

Bank for International Settlements (2005). Zero-coupon yield curves: Technical documentation. Technical Report 25, Bank for International Settlements, Basel.

Brüggemann, R., Jentsch, C., and Trenkler, C. (2016). Inference in VARs with conditional heteroskedasticity of unknown form. *Journal of Econometrics*, 191(1):69–85.

Campbell, J. Y. and Shiller, R. J. (1991). Yield spreads and interest rate movements: A bird's eye view. *The Review of Economic Studies*, 58(3):495–514.

Campbell, J. Y., Shiller, R. J., and Viceira, L. M. (2009a). Understanding inflation-indexed bond markets. *Brookings Papers on Economic Activity*, 2009(1):79–120.

Campbell, J. Y., Sunderam, A., and Viceira, L. M. (2009b). Inflation bets or deflation hedges? The changing risks of nominal bonds. Working Paper 14701, National Bureau of Economic Research. Revised July 2013.

Christensen, J. H. E., Lopez, J. A., and Rudebusch, G. D. (2010). Inflation expectations and risk premiums in an arbitrage-free model of nominal and real bond yields. *Journal of Money, Credit and Banking*, 42(S1):143–178.

Cochrane, J. H. (2005). Term structure of interest rates. In *Asset Pricing*, chapter 19, pages 349–382. Princeton University Press, Princeton, New Jersey, revised edition.

D'Amico, S., Kim, D. H., and Wei, M. (2018). Tips from TIPS: The informational content of Treasury inflation-protected security prices. *Journal of Financial and Quantitative Analysis*, 53(1):395–436.

Diebold, F. X. and Li, C. (2006). Forecasting the term structure of government bond yields. *Journal of Econometrics*, 130(2):337–364.

Driscoll, T. A. and Braun, R. J. (2017). Piecewise interpolation. In *Fundamentals of Numerical Computation*, chapter 5. Society for Industrial and Applied Mathematics. Accessed: 2026-03-15.

Duffee, G. R. (2002). Term premia and interest rate forecasts in affine models. *The Journal of Finance*, 57(1):405–443.

Duffie, D. and Kan, R. (1996). A yield-factor model of interest rates. *Mathematical Finance*, 6(4):379–406.

Evans, M. D. D. (1998). Real rates, expected inflation, and inflation risk premia. *The Journal of Finance*, 53(1):187–218.

Fama, E. F. (1990). Term structure forecasts of interest rates, inflation, and real returns. *Journal of Monetary Economics*, 25(1):59–76.

Fama, E. F. and Bliss, R. R. (1987). The information in long-maturity forward rates. *The American Economic Review*, 77(4):680–692.

Gürkaynak, R. S., Sack, B., and Wright, J. H. (2007). The U.S. treasury yield curve: 1961 to the present. *Journal of Monetary Economics*, 54(8):2291–2304.

Gürkaynak, R. S., Sack, B., and Wright, J. H. (2010). The TIPS yield curve and inflation compensation. *American Economic Journal: Macroeconomics*, 2(1):70–92.

Hördahl, P. and Tristani, O. (2012). Inflation risk premia in the term structure of interest rates. *Journal of the European Economic Association*, 10(3):634–657.

Künsch, H. R. (1989). The jackknife and the bootstrap for general stationary observations. *The Annals of Statistics*, 17(3):1217–1241.

Litterman, R. and Scheinkman, J. A. (1991). Common factors affecting bond returns. *Journal of Fixed Income*, 1:54–61.

Mishkin, F. S. (1990). What does the term structure tell us about future inflation? *Journal of Monetary Economics*, 25(1):77–95.

Nelson, C. R. and Siegel, A. F. (1987). Parsimonious modeling of yield curves. *The Journal of Business*, 60(4):473–489.

Pflueger, C. E. and Viceira, L. M. (2013). Return predictability in the Treasury market: Real rates, inflation, and liquidity. Working Paper 16892, National Bureau of Economic Research.

Piazzesi, M. (2010). Affine term structure models. In Aït-Sahalia, Y. and Hansen, L. P., editors, *Handbook of Financial Econometrics: Tools and Techniques*, chapter 12, pages 691–766. Elsevier.

Piazzesi, M. and Schneider, M. (2006). Equilibrium yield curves. In Acemoglu, D., Rogoff, K., and Woodford, M., editors, *NBER Macroeconomics Annual*, volume 21, pages 389–472. MIT Press.

Svensson, L. E. O. (1994). Estimating and interpreting forward interest rates: Sweden 1992–1994. *National Bureau of Economic Research Working Paper*, 4871.

Appendix

A1: Zero-coupon yield data

Term structure models impose a functional relationship between interest rates and term to maturity. In parametric term structure models, the shape of the yield curve is assumed governed by a set of parameters which are calibrated to minimize the price or yield fitting errors with respect to observed bonds. This is possible because coupon bonds are priced as portfolios of zero-coupon bonds where each coupon is discounted by the corresponding zero-coupon yield. When selecting a model, there is a trade-off between including a large set of parameters, which might ensure perfect fit, and obtaining a smoother yield curve which preserves a higher degree of economic interpretation of the shape of the curve. In practice, there are several factors that cause idiosyncratic pricing at different maturities, ruling out perfectly smooth yield curves. This for instance includes higher demand for bonds that are deliverable into SGB futures contracts. Because our objective is macroeconomic analysis, we are not interested in capturing these idiosyncrasies. We therefore adopt a parsimonious model where a few parameters characterize the entire yield curve. Svensson (1994) extends the Nelson and Siegel (1987) assumed form of the instantaneous forward rate:

$$f_t(n,0) = \beta_{t,0} + \beta_1 \exp(-\frac{n}{\tau_1}) + \beta_2 \frac{n}{\tau_1} \exp(-\frac{n}{\tau_1}) + \beta_3 \frac{n}{\tau_2} \exp(-\frac{n}{\tau_2}), \tag{24}$$

where $\beta_0, \beta_1, \beta_3, \tau_1$ and τ_2 are parameters to estimate. $f_t(n,0)$ is the continuously compounded interest rate on a forward contract at trade date t, with effective date $t+n$ and an infinitesimal investment period $m \to 0$. The m-period interest rate is the average of the instantaneous forward rates between t and m, $y_t(m) = \frac{1}{m}\int_0^m f_t(n,0)dn$. Integrating (24) gives

$$\begin{aligned} y_t^{(m)} = \\ \beta_0 + \beta_1 \frac{1-\exp\left(-\frac{m}{\tau_1}\right)}{\frac{m}{\tau_1}} + \beta_2 \left(\frac{1-\exp\left(-\frac{m}{\tau_1}\right)}{\frac{m}{\tau_1}} - \exp\left(-\frac{m}{\tau_1}\right) \right) \\ + \beta_3 \left(\frac{1-\exp\left(-\frac{m}{\tau_2}\right)}{\frac{m}{\tau_2}} - \exp\left(-\frac{m}{\tau_2}\right) \right). \end{aligned} \tag{25}$$

Interest rates and forward rates approach β_0 as maturity approaches infinity. The intercept of the curve is given by $\beta_0 + \beta_1$ for $m = 0$. The third term allows for a hump of magnitude β_2 in the forward curve and $\tau_1 > 0$ determines where the hump reaches its maximum. Svensson (1994) adds the fourth term to allow for a second hump which is often present at long end of the yield curve. The Nelson and Siegel (1987) model is obtained by setting $\beta_3 = 0$. The loading with respect to maturity on β_0 is constant while the loading on β_1 monotonically goes to zero. The loadings on β_2 and β_3 start at zero, increase and then end at zero. The Nelson-Siegel curve can therefore intuitively be characterized by level, slope and curvature factors (Diebold and Li, 2006).

A1.1 Price data and the indexation-lag

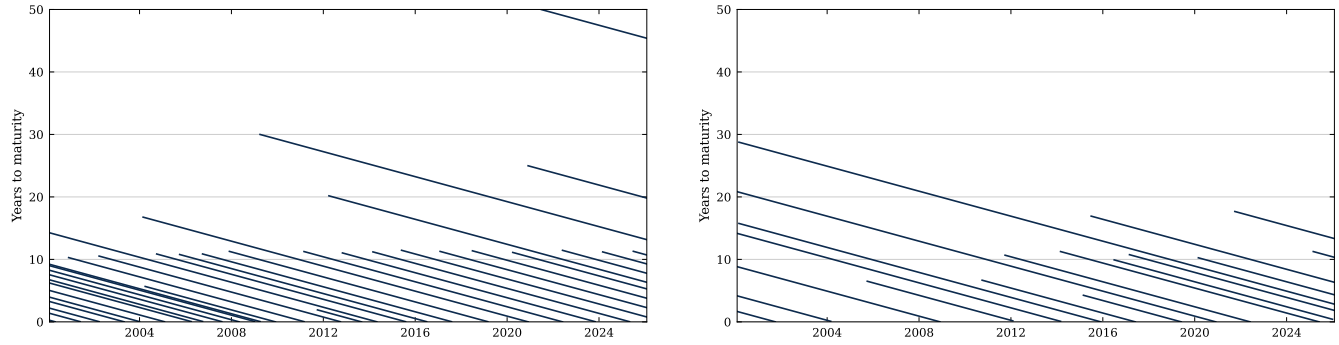
We collect prices at close from the last trading day of each month between 2000 and 2025 for outstanding SGBs and SGBis available in Bloomberg. Bonds prices reflect the present value of

future coupon and principal payments. For inflation-linked bonds, these cash flows are indexed to the CPI published by Statistics Sweden. These bonds are issued with a base-index equal to the CPI three months prior to the first settlement date of the bond. Over the term of the bond, inflation compensation is accrued according to an index factor which is the ratio of the current reference index and the base index. The reference index for the first day of the month equals the CPI three months earlier. For any other day in the month, the reference index is calculated by linear interpolation between the CPI three months and two months prior, assuming 30-day months. The reference index of an inflation-linked bond traded at time t with settlement at day d_t the current month m is therefore $Q_t = CPI_t(m-3) + \frac{d_t-1}{30}\Big(CPI(m-2) - CPI_t(m-3)\Big)$. The three month lag in the reference index is referred to as the *indexation lag*. Due to the indexation lag, bondholders receive compensation for inflation during the three months before the purchase. Further, they receive no compensation for the inflation during the final three months of the holding period.

The quoted SGBi prices we collect from Bloomberg contain accrued inflation compensation. The holder of an inflation-linked bond receives the specified nominal cash flows of the bond scaled by the relevant index factors. For example, if a bond has a nominal coupon c_t, then $c_t \times \frac{Q_t}{Q_0}$ is the cash flow received by the bondholder, where Q_0 is the base-index of the bond. Clean SGBi prices are obtained by dividing quoted prices by the current index factor. The clean price of an inflation-linked bond with m years to maturity that is traded at t is computed as:

$$P^{(m)}_{t,clean} = P^{(m)}_{t,quoted} / \frac{Q_t}{Q_0}. \tag{26}$$

We compute clean SGBi prices from our sample of quoted Bloomberg SGBi prices according to equation (26). We use CPI series with base year 1980 collected from Statistics Sweden (SCB) for this purpose.



(a) SGB (b) SGBi

Figure 10: Swedish government bonds outstanding, 2000–2025. Outstanding SGBs and SGBis are plotted by time left to maturity in years. *Source: Authors' rendering of Bloomberg data (2000–2025).*

A1.2 Estimation

The total number of outstanding bonds in our data are plotted in figure 10. Parametric yield curves are prone to exhibit poor fit at the front end of the curve as bonds tend to

become less traded when they near maturity. For this reason, we exclude SGBs with less than three months to maturity from the sample, similar to Gürkaynak et al. (2007). To facilitate identification of short SGB yields, we include zero-coupon yields at 1, 3 and 6 month maturities from the Swedish T-Bill curve estimated by the Riksbank, available at daily frequency through their API. Since long-dated bonds tend to be significantly less traded we drop nominal bonds with more than fifteen years to maturity from the sample. The short end of the inflation-linked yield curve can be subject to meaningful distortions from the three month indexation lag. Estimating the US TIPS yield curve, Gürkaynak et al. (2010) exclude TIPS with shorter than 1.5 years to maturity and down-weight TIPS with between 1.5 and 2 years to maturity in estimation to limit the impact of the indexation-lag. In section 5, we estimate arbitrage-free inflation-linked yield curves for maturities from 2 to 10 years. Because there are few outstanding short maturity SGBis, we exclude SGBis with maturities shorter than 1 year to avoid severe extrapolation at the short end of the curve in many of the cross sections in our empirical analysis (section 5). Extrapolation is still present however, with the shortest maturity SGBi in our sample during the periods 2007-12 to 2010-05 and 2021-06 to 2022-05 for instance ranging being between 3-4 years. We avoid extrapolating the long end of the SGBi curve entirely by including bonds with maturities shorter than 20 years. It is important to note that the difficulties to pin down the short and long ends of the SGBi curve negatively impacts the reliability of our results. Finally, because there were only 4 to 5 outstanding SGBis that satisfy these criteria before 2006-01, we restrict our sample to only cover the period 2006-01 to 2025-12.

Because many cross-sections contain under identified segments, especially for SGBis, we take several steps to improve the stability of the parameter estimates. First, we decide to use the Nelson-Siegel-Svensson (NSS) form in (25) to estimate the nominal yield curve, and the Nelson-Siegel (NS) form for the inflation-linked curve. NS requires estimating four parameters, compared to six parameters in NSS. The NS model, which only allows for one hump, is unable to fit excessive curvature at both ends of the yield curve. In the analysis, we do not use inflation-linked yields shorter than two years which makes poor identification of short end curvature less of an issue.

Second, we include artificial zero-coupon bonds at the midpoints between each pair of adjacent bonds from bootstrapped yield curves. Starting with the shortest maturity bond, bootstrapped zero-coupon yields are solved sequentially such that the yield curve exactly reprices the observed bonds by recursively applying bond pricing formulas. Prices are given by $P_t^{(m)} = \sum_{i=0}^{n} CF_i D_t^{(i)}$, where $D_t^{(i)}$ is the i-period discount factor. A cross section with n bonds is divided into n-segments connecting n nodes on the discount curve $D_t^{(m)}$. Because cash flows do not occur at fixed time intervals, we cannot apply the pricing formula directly to solve for the yield at each node. Instead, the discount function over each segment must be interpolated in a way that generates exact prices. The discount function is fitted by a cubic spline, meaning that cubic polynomials are fitted to each segment and jointly create a continuous global polynomial defined over the entire observed domain. The cubic polynomials are restricted such that the first two derivatives and levels are identical at each node, ensuring uniquely determined coefficients and global smoothness of the discount function. We prefer the cubic form over a piecewise linear interpolant, which also generates exact bond pricing but

with discontinuities at the node points (see e.g. Driscoll and Braun (2017)). Bootstrapping solves for the discount factors at each node, conditional on the form of the interpolated curve. This must be done sequentially and the cubic spline is recomputed at each stage given the current nodes. We use the PiecewiseLogCubicDiscount function in the QUANTLIB library in Python, which fits the logarithm of the discount factor to guarantee positive discount factors. The bootstrapped discount factors are used to construct the artificial zero-coupon yields. The shape of the bootstrapped curve is locally determined which makes the artificial bonds less influenced by functional form assumptions. It is still worth noting that the synthetic bonds do not add any new information and the final yield curve estimation could import bias from a potentially poorly fitted bootstrapped curve.

The final yield curve estimation is performed with QUANTLIB in Python. The yields implied by a given set of parameter values in equation (25) are used to price the bonds in the cross section. Parameter estimation is achieved by minimizing sum of squared pricing errors. Because the prices of long maturity bonds are more sensitive to changes in the yield compared to short maturity bonds, minimizing price errors tend to overfit long term yields at the expense of short term yield fit (see discussion in Bank for International Settlements (2005)). For this reason, prices are weighted by the inverse duration of the bonds. Starting values of the parameters are chosen to mitigate the risk that the optimizer gets stuck in local minima. The starting values for β_0 are the zero-coupon yields from the longest maturity on the nominal and inflation-linked bootstrapped curves, respectively. For nominal bonds, the starting value for $\beta_0 + \beta_1$ is set to the Riksbank's deposit rate. There exists no real deposit rate to use for inflation-linked bonds. We instead use the one month yield from the Riksbank's estimated Swedish T-bill curve minus 12-month trailing CPI inflation as a proxy for the real deposit rate. Finally, we run the estimation using different combinations of economically plausible starting values for β_2, β_3, τ_1 and τ_2 and select the specifications that minimize the objective. We include light penalties on deviations from the starting values improve parameter stability. The time series of the estimated nominal and inflation-linked term structures are plotted in figure 11.

Figure 12 plots the root mean squared yield fitting errors (RMSE) in basis points (bp) from repricing the observed SGBs and SGBis in the sample from the estimated yield curves. Nominal fitting errors are higher in the beginning of the sample, often reaching 8 bp, then fall to 2-4 bp between 2014 to 2022, and exhibit a temporary spike around 2022-2023, when interest rates rose sharply. The fitting errors for inflation-linked bonds are generally lower, but exhibit a similar pattern as nominal bonds. To some extent, the fitting errors tend to rise when the shape of the yield curve changes. Both graphs spike around 2009, when short term bond yields fell, and in 2022-2023 when they rose. Lower RMSEs for SGBis compared to SGBs is likely an effect of fewer bonds outstanding, rather than evidence that the inflation-linked yield curve is better identified, as it may be easier to fit a smooth curve when there are fewer bonds to take into account. The small fitting errors for inflation-linked bonds may in fact indicate a higher degree of overfitting on noise. Overfitting also helps to explain the occasionally erratic pattern of fitting errors present in both curves. Dashed line RMSEs are computed from yield curves fitted solely on observed bonds, while the blue lines show the fitting errors from yield curves that are estimated with the artificial bootstrapped bonds,

as we documented earlier. The fitting errors from the actual and extended curves are near indistinguishable, indicating that the artificial bonds improve parameter stability, without introducing additional local bias to the fit. Figure 13 plots the fitting errors by maturity bins. It is evident that most nominal fitting errors stem from the short end of the curve. By the addition of three estimated T-Bill yields to each nominal cross section, one can argue that the short end of the nominal yield curve is the best identified segment on any curve. This would imply that there is persistent overfitting at the longer end of the curves. The size of the fitting errors however indicates that part of the short-end fitting errors also stems from genuine difficulties for the optimizer to identify short term nominal yields.

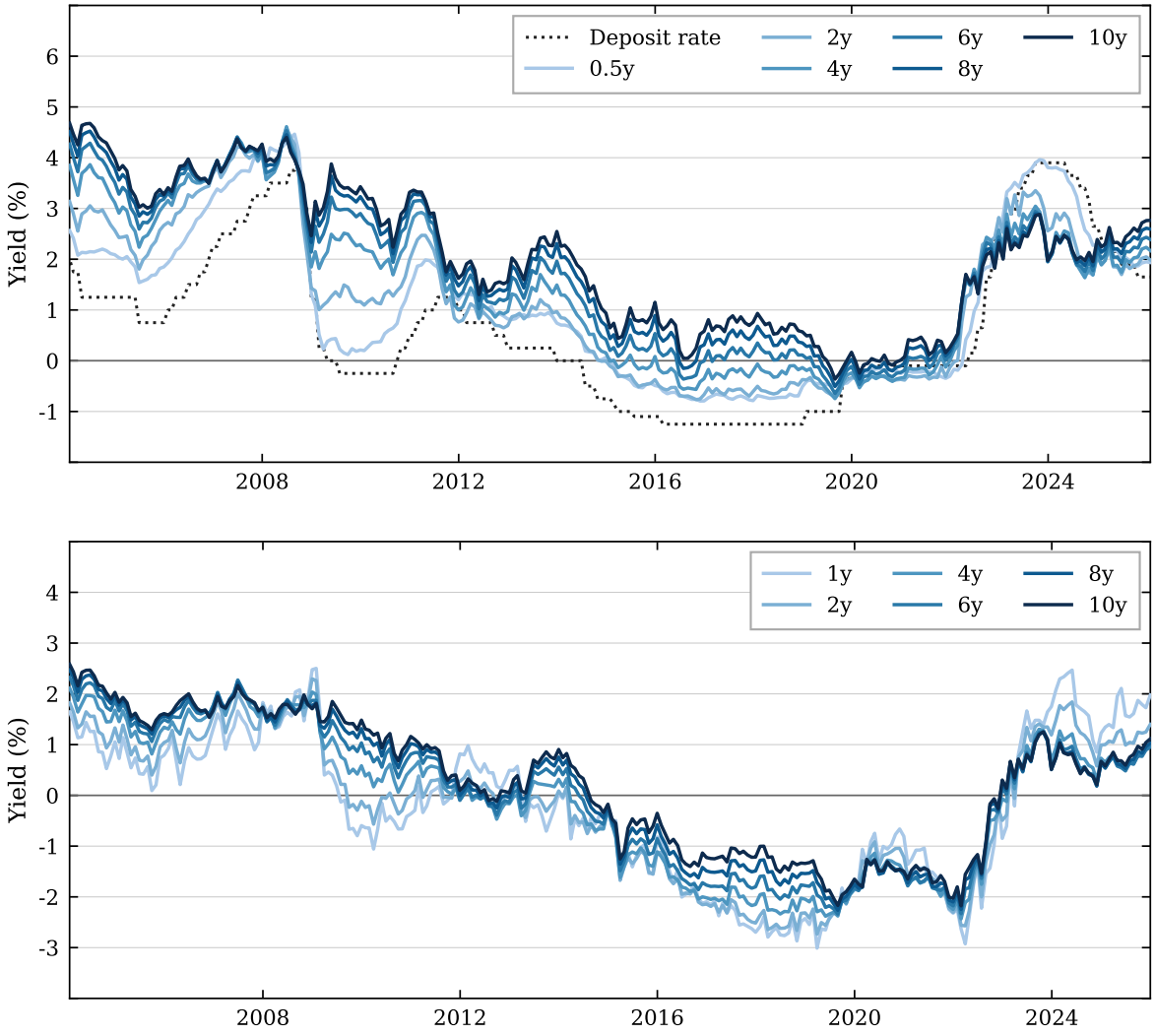


Figure 11: *Top:* Time series of estimated nominal NSS curves at selected maturities and the Riksbank's deposit rate. *Bottom:* Time series of estimated inflation-linked NS curves at selected maturities. *Source: Authors' calculations based on Riksbank and Bloomberg data (2006–2025).*

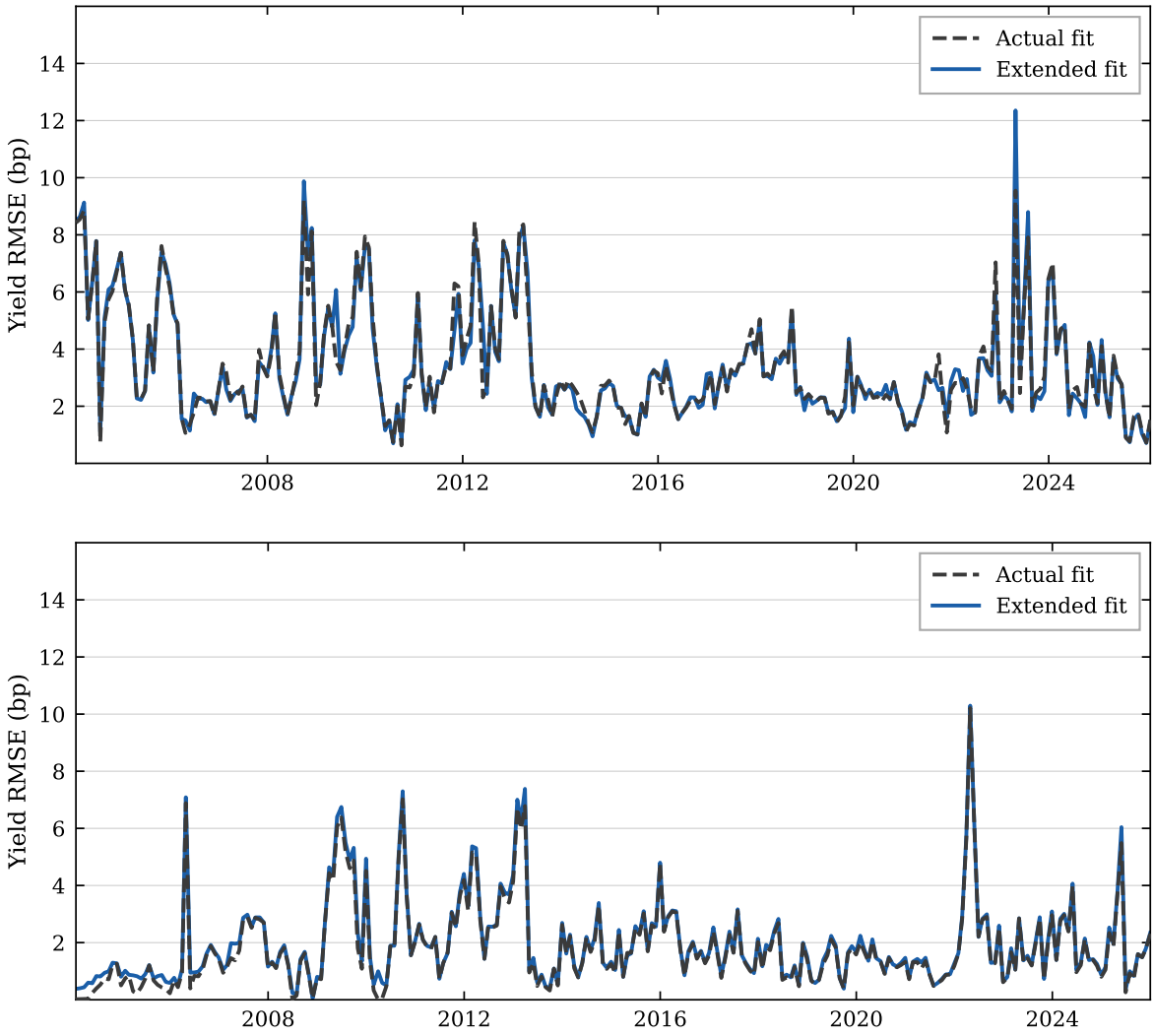


Figure 12: *Top:* Time series of root mean squared nominal yield fitting errors *Bottom:* Time series of root mean squared inflation-linked yield fitting errors. Actual fit (dashed) is based only on actual bond data. In the extended fit (line), artificial bootstrapped yields are included. RMSE is computed only with regards to actual SGB and SGBi bonds. *Source: Authors' calculations based on Riksbank and Bloomberg data (2006–2025).*

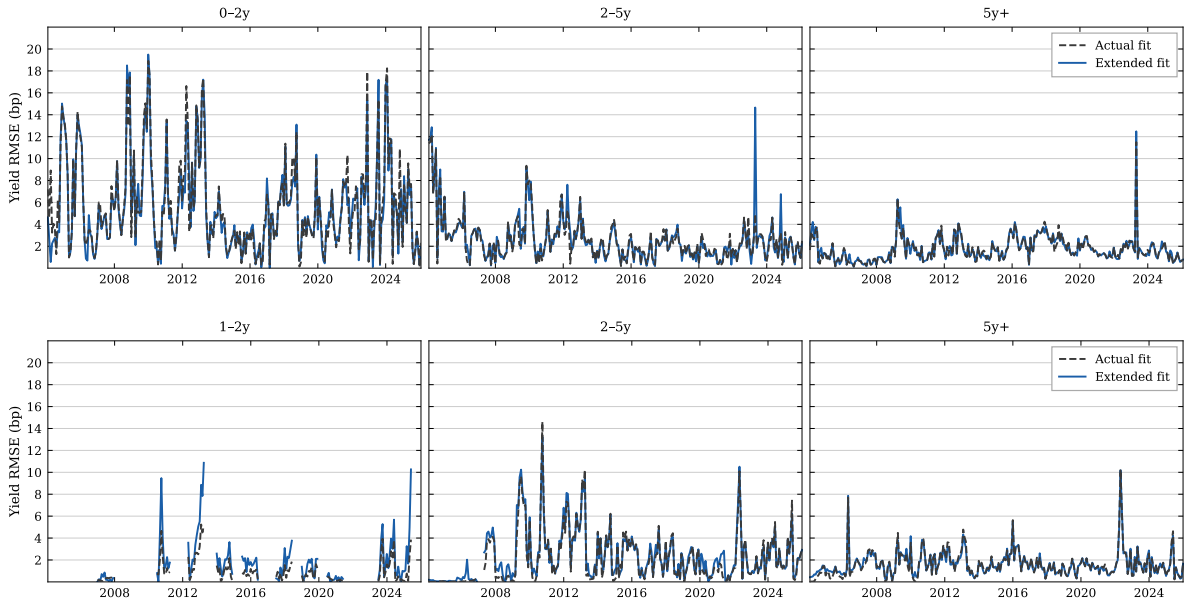


Figure 13: *Top:* Time series of root mean squared nominal yield fitting errors by maturity. *Bottom:* Time series of root mean squared inflation-linked yield fitting errors by maturity. *Source: Authors' calculations based on Riksbank and Bloomberg data (2006–2025).*

Appendix A2: Additional tables and graphs

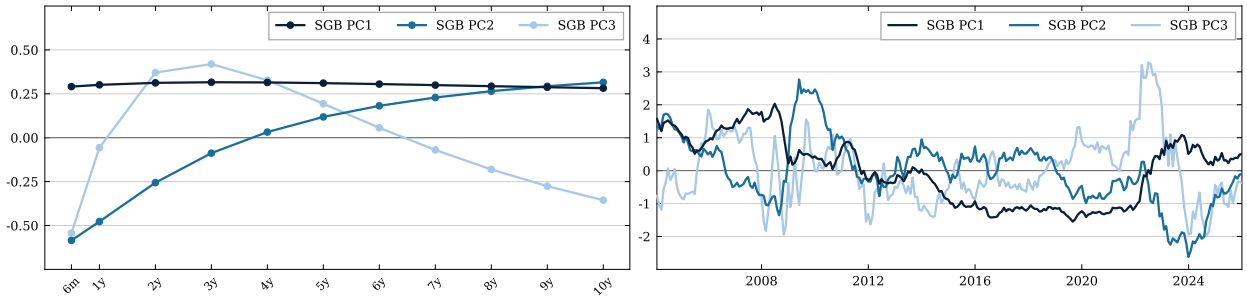


Figure 14: **Nominal SGB principal components, five-factor Specification.** *Left:* Factor loadings of the three nominal principal components across maturities from 6 months to 10 years. *Right:* Evolution of the factor scores over the sample period. *Source: Authors' calculations based on Bloomberg data (2006–2025).*

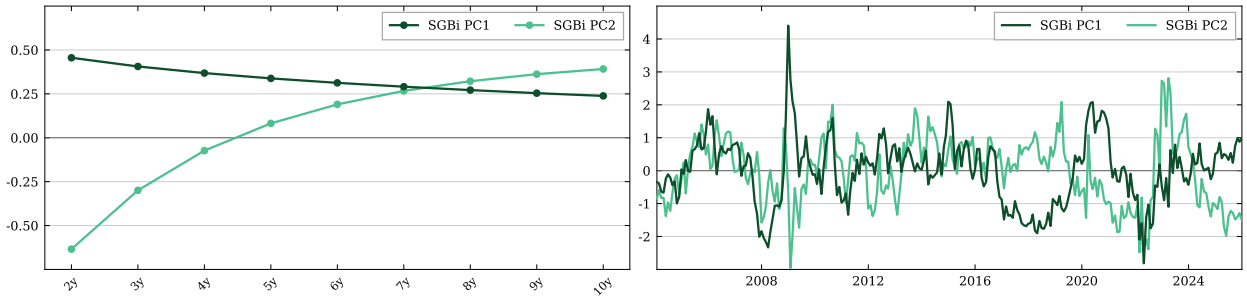


Figure 15: **Inflation-linked principal components, five-factor specification.** *Left:* Factor loadings of PC4_R and PC5_R across maturities from 2 to 10 years. *Right:* Evolution of the PC4_R and PC5_R factor scores over the sample period. *Source: Authors' calculations based on Bloomberg data (2006–2025).*

	Yield fitting error (bp)					Excess return fitting error (bp)				
Maturity	Mean	Std.	RMSE	$\rho(1)$	$\rho(6)$	Mean	Std.	RMSE	$\rho(1)$	$\rho(6)$
Panel A: Nominal bonds										
2Y	1.11	4.99	5.11	0.77	0.24	0.11	7.12	7.12	−0.19	0.03
5Y	−0.25	4.74	4.75	0.92	0.69	−0.11	9.32	9.32	−0.16	0.05
10Y	2.57	5.54	6.11	0.76	0.21	0.27	38.20	38.20	−0.19	0.02
Panel B: Inflation-linked bonds										
2Y	0.88	8.79	8.83	0.91	0.60	−0.15	7.88	7.88	−0.02	−0.01
5Y	−3.12	3.66	4.81	0.74	0.26	−0.41	13.01	13.01	−0.12	−0.01
10Y	−0.10	5.77	5.77	0.85	0.51	0.49	30.93	30.94	−0.07	−0.03

Table 7: **Fit diagnostics, five-factor specification.** Yield fitting errors (bp) and model-implied excess return fitting errors (bp) at selected maturities. Mean, standard deviation, and RMSE are reported for yield pricing errors (observed minus model-implied zero-coupon yields) and for excess return pricing errors (actual minus model-implied one-month holding period returns from the pricing recursion). $\rho(1)$ and $\rho(6)$ denote first- and sixth-order autocorrelations of the respective error series. *Source: Authors' calculations based on Bloomberg and Statistics Sweden (SCB) data (2006–2025).*

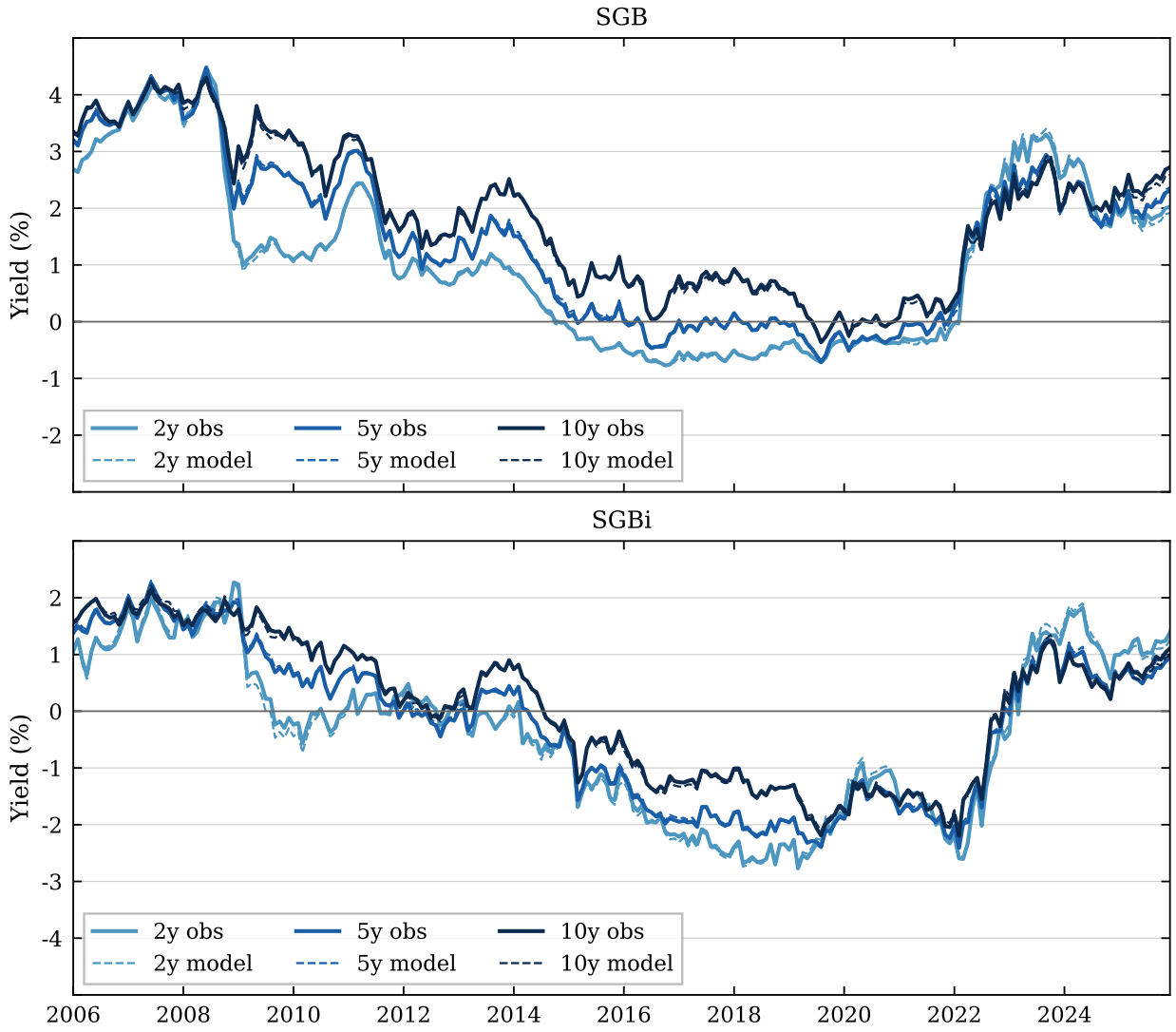


Figure 16: **Observed and model-implied zero-coupon yields, five-factor specification.** Solid lines are observed yields and dashed lines model-implied yields at the 2-, 5-, and 10-year maturities. The upper panel shows SGBs and the lower panel shows SGBis. *Source: Authors' calculations based on Bloomberg and Statistics Sweden (SCB) data (2006–2025).*

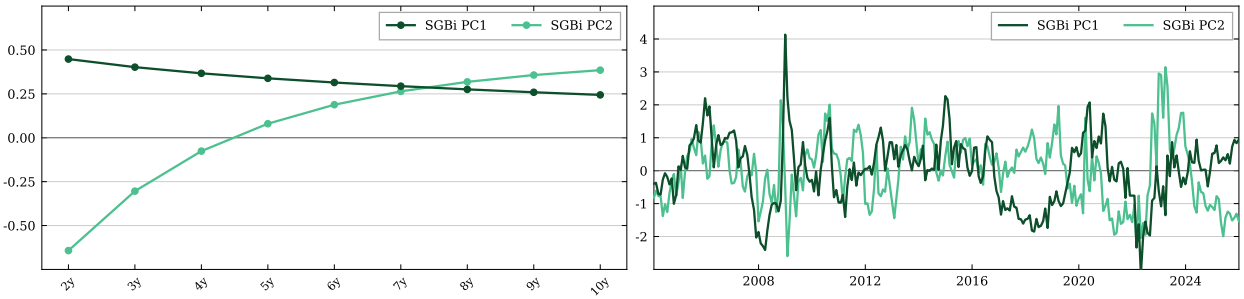


Figure 17: **Inflation-linked principal components, six-factor specification.** *Left:* Factor loadings of $PC4_R$ and $PC5_R$ across maturities from 2 to 10 years. *Right:* Evolution of the $PC4_R$ and $PC5_R$ factor scores over the sample period. *Source: Authors' calculations based on Bloomberg, Statistics Sweden (SCB), FRED, and SNDO data (2006–2025).*

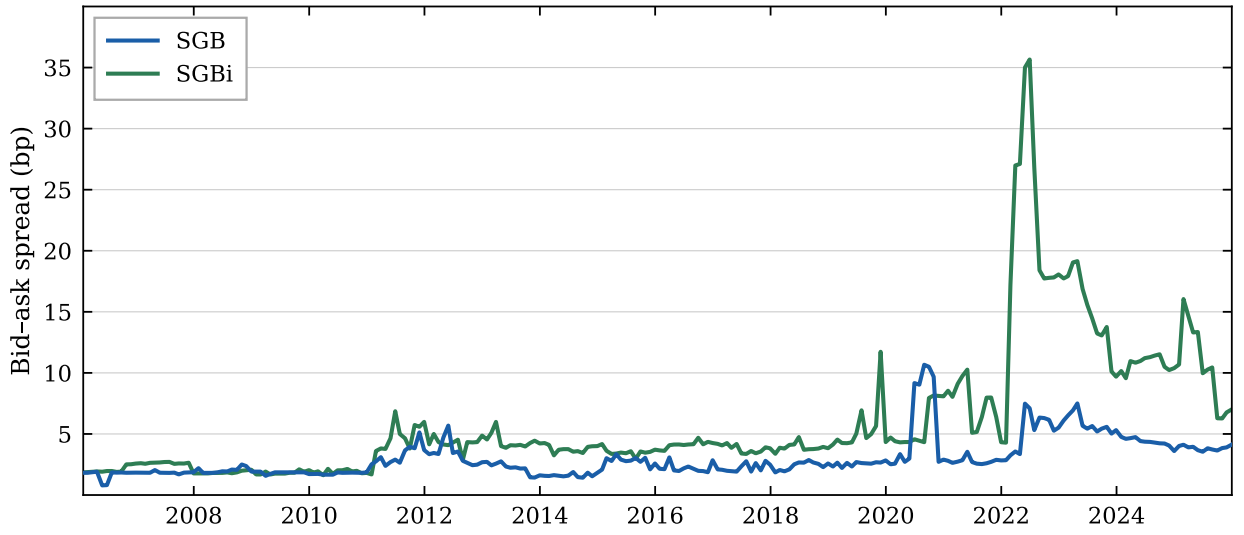


Figure 18: Implied mean bid-ask yield spreads for SGB and SGBi securities with maturities between 1 year and 10 years. *Source: Authors' rendering of Bloomberg data (2006–2025).*

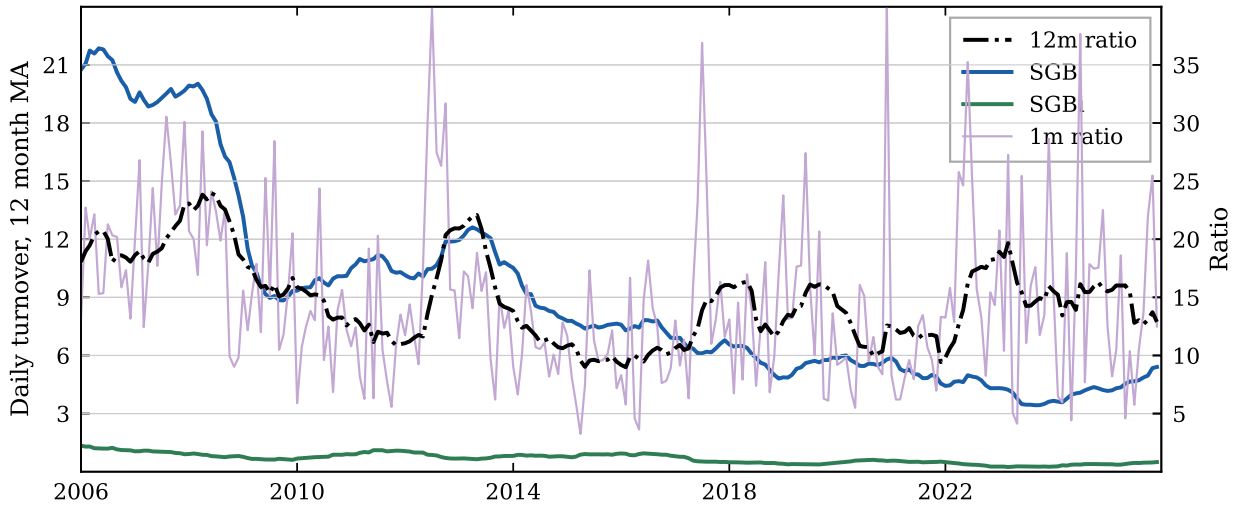


Figure 19: *LHS:* Twelve-month moving average of daily secondary market turnover from investors and market dealers (bn SEK) for SGB and SGBi securities. *RHS:* Twelve-month ans one-month turnover ratios. *Source: Authors' rendering of SNDO data (2006–2025).*